University of Michigan

College of Literature, Science and the Arts

The role of the chemokine receptor CXCR7 in glioblastoma progression

By: Sriakhila Akula

Mentor: Anda-Alexandra Calinescu, MD, PhD

Research Assistant Professor, Department of Neurosurgery

Reader 1: Sara Aton, PhD

Assistant Professor, Department of Molecular, Cellular, and Developmental Biology

Reader 2: Bo Duan, PhD

Assistant Professor, Department of Molecular, Cellular, and Developmental Biology

A thesis submitted in partial fulfilment of the

Degree of Bachelor of Science in Neuroscience with Honors

April 15, 2020

Abstract

Glioblastoma (GB) is one of the deadliest and most common forms of primary malignant brain tumors. Glioblastoma Stem Cells (GSCs), a small population of cells present in the tumor, cells that are resistant to chemo- and radiotherapy, contribute significantly to treatment failure and disease recurrence. Previous studies have demonstrated an important role for the chemokine CXCL12 in survival and proliferation of GSCs and in promoting GB progression. CXCL12 can bind to two G-protein coupled receptors: CXCR4, the main signaling receptor for CXCL12 and CXCR7, an atypical chemokine receptor, considered to function as a decoy receptor that sequesters CXCL12 and decreases signaling through CXCR4. Most studies to date have analyzed the effects of CXCR4 activation by CXCL12. Few studies have tested the role of CXCR7 in GB, and some of these portray conflicting results. Experiments presented herein address the role of CXCR7 in GB progression by analyzing the growth dynamics, response to CXCR4 and CXCR7 inhibitors and production of CXCL12 in GSCs and GSCs overexpressing CXCR7 (GSC-X7). *In vitro* growth analysis demonstrated that GSC-X7 have an increased proliferative capacity especially after prolonged time in culture. GSC-X7 exhibited an increased resistance to treatment with small molecule inhibitors of CXCR4 (AMD3100) and CXCR7 (CCX771) and increased expression of *Cxcl12* after prolonged time in culture. Combinatorial treatment with AMD3100 and CCX771 reduced the viability of GSCs the most, still significantly less in CXCR7 expressing GSCs when compared to their parental cell line. Taken together, these results confirm an important role of CXCL12 in the biology of GSCs and suggest that CXCL12 expression is controlled by a complex autocrine feedback mechanism, regulated in part through levels of CXCR7. Further experiments will dissect the molecular and cellular mechanisms that govern regulation of CXCL12 production by CXCR7 in GSCs. In addition, a thorough *in vivo* analysis of tumor progression using GSC and GSC-X7 will ascertain if expression of CXCR7 on GSCs promotes GB progression. A detailed understanding of the mechanisms that govern CXCL12 biology in GSCs will allow the design of specific therapeutic agents to target GSCs.

Table of Contents

Scientific Acknowledgments

Figure #	Person who was responsible for the illustrated experiment
Supplementary Fig. 1	I generated the lentiviral vector using subcloning methods.
Supplementary Fig. 2	The data was collected and analyzed by me.
Supplementary Fig. 3	The data was collected and analyzed by me.
Supplementary Fig. 4	The data was collected and analyzed by me.
Supplementary Fig. 5	The resulting vector was generated and analyzed by me.
Fig. 4	The data was collected by Dr. Calinescu and analyzed by Dr. Calinescu and me.
Table 1	The data was collected and analyzed by me.
Fig. 5	The data was collected by Dr. Calinescu and analyzed by me.
Fig. 6, Table 2	The data was collected by Georgia Tapsall and Dr. Calinescu and analyzed by Dr. Calinescu and me.
Fig. 7	The data was collected and analyzed by me.
Fig. 8, Table 3	The data was collected by Dr. Calinescu and analyzed by Dr. Calinescu and me.
Fig. 9	The data was collected and analyzed by me.
Fig. 10	The data was collected and analyzed by me.
Fig. 11	The data was collected and analyzed by Dr. Calinescu, Eric Hsieh and me.

Personal Acknowledgments

I would like to show my sincere gratitude to my mentor, Dr. Alexandra Calinescu, for supporting me through the data collection/analysis and the thesis writing process. I really appreciate the immense amount of patience she exhibits while answering all my questions. She has been a major pillar of support throughout my undergraduate education by reminding me of my strengths. She has been one of the few people to consistently believe that I can achieve great things in life and will pursue my dreams. I am forever indebted to her for the continuous words of encouragement, guidance, and unconditional support for the past two years inside and outside the lab. Her kind words of encouragement reinforced my passion to pursue medicine. In addition, her determination to push me beyond my limits with this thesis has reignited my scientific curiosity. I hope to take with me your kind words of wisdom beyond my undergraduate degree.

In addition, I would like to thank Eric Hsieh and Georgia Tapsall for helping me collect data and supporting my undergraduate thesis journey. The help of these two individuals made the data collection process much smoother.

Finally, I would like to thank my parents for showing unconditional love and encouragement throughout my life. They have been a strong backbone for me in all of my pursuits. I am grateful that they let me chase my dreams to pursue science and medicine especially in a family full of engineers. They have believed in me more than I have believed in myself.

Introduction

Overview of Glioblastoma

Primary brain tumors are one of the top ten cancer-related deaths in North America and Europe (Agnihotri et al., 2013). Among primary brain tumors, gliomas are the most common malignant tumors with an incidence of 6 per 100,000 population (2010-2014) (Ostrom et al., 2018). The majority of gliomas (61.5%) are glioblastomas (GB), the most aggressive form of brain tumors, a disease without cure. Although current therapies slow progression, the 5-year survival rate for patients diagnosed with GB remains at around 5% and the median life expectancy at 15-17 months after diagnosis (Ostrom et al., 2016). The current standard of care for patients treated for GB includes tumor resection followed by radiation therapy and chemotherapy with Temozolomide, an alkylating cytotoxic drug (Stupp et al., 2005).

In addition to the standard of care, other treatment options including anti-angiogenic therapies with antibodies against the vascular epithelial growth factor A (VEGF-A), inhibition of Receptor Tyrosine Kinases, like EGFR, FGFR, PDGFR as well as immunotherapy to promote the antitumor immune response have been tried, with little benefit so far, to the overall survival of patients. (Hottinger et al., 2014; Neilsen et al., 2019). Most recently, addition of tumor treating fields (TTF), an antimitotic treatment delivered by means of alternating electric fields via transducer arrays applied to the scalp of patients, has been shown to increase progression and overall survival in GB patients from 4 months to 6.7 months and from 16 months to 20.9 months, respectively (Stupp et al., 2005).

The first classification of tumors of the nervous system published by the World Health Organization (WHO) in 1979, and the subsequent editions up to 2007, classified brain tumors primarily on histological criteria, morphological and immuno-histochemical features, according to the presumed cell of origin and an added tumor grading (I-IV) indicating the severity of the disease. (Weller et al., 2019). Based on extensive studies indicating diagnostic and prognostic value of genetic and epigenetic alterations of different brain tumors, as well as the realization that the cell of origin of high grade gliomas is still unknown, the 2016 WHO classification of tumors includes a combination of histological and molecular characteristics for the definition of the different brain tumor entities. Brain tumors with the worst prognosis are WHO grade IV malignant tumors, encompassing: diffuse anaplastic astrocytomas, glioblastomas that can be either IDH mutant or wild-type, diffuse midline glioma with mutation in Histone 3 (H3-K27M),

anaplastic oligodendrogliomas IDH mutant, with or without co-deletions of chromosomes 1p/19q as well as embryonal tumors (Weller et al., 2019).

Primary GBs form rapidly growing tumors within the parenchyma of the forebrain, tumors that are highly invasive, intensely vascularized, composed of a heterogeneous population of malignant cells and infiltrating immune cells. Characteristic histological features of GB are the presence of pseudopalisades: necrotic areas surrounded by columns of outward migrating tumor cells, diffuse invasion into the brain parenchyma, nuclear atypias, microvascular proliferations, glomeruloid vascular abnormalities and regions of hemorrhage (Rojiani and Dorovini-Zis, 1996; Holland, 2001). Following the standard of care, GB invariably recur and progress to an increasingly more aggressive form of the disease, recurrence attributed to the heterogeneous makeup of the tumors, making them difficult to target with single agents, the presence of the blood-brain-barrier and abnormal intra-tumoral vascularization, that prevents optimal drug penetration and the presence of glioma stem cells (GSCs), that are resistant to chemo- and radiotherapy.

Common genetic alterations present in Gliomas

Several genetic alterations have been commonly identified in gliomas, some of which show prognostic value and correlate with clinical grade. Overexpression of growth factors and their receptors: platelet derived growth factor (PDGF), fibroblast growth factor (FGF) and ciliary neurotrophic growth factor (CNTF), as well as mutations in the TP53 tumor suppressor gene have been documented in lower grade gliomas. In grade III anaplastic gliomas, mutations in genes regulating cell cycle progression, like deletions or mutations of the Cyclin Dependent Kinase Inhibitor 2A (CDKN2A) and CDKN2B genes, amplification of the Cyclin Dependent Kinase 4 (CDK4) gene or loss of the Retinoblastoma (RB) tumor suppressor gene are common. Grade IV gliomas in addition show frequent loss of the chromosomal region 10q22-25 which encodes the tumor suppressor gene Phosphatase and Tensin Homologue (PTEN), an inhibitor of the AKT kinase and part of the PI3K pathway, that promotes proliferation, cell survival and angiogenesis in numerous tumors (Holland, 2001; Neilsen et al., 2019). Other mutations of genes in the Receptor Tyrosine Kinase (RTK)/RAS/PI3K pathway, namely mutations in PI3CA and PIK3R1, have also been described (Network, 2008). A summary diagram of the three main signaling pathways: RTK/RAS/PI3K, TP53 and the RB pathway, that harbor the most common

genetic alterations identified in GB is presented in **Figure 1,** adapted from The Cancer Genome Atlas Research Network article (Network, 2008).

Amplification of the epidermal growth factor receptor gene (EGFR) with gain of
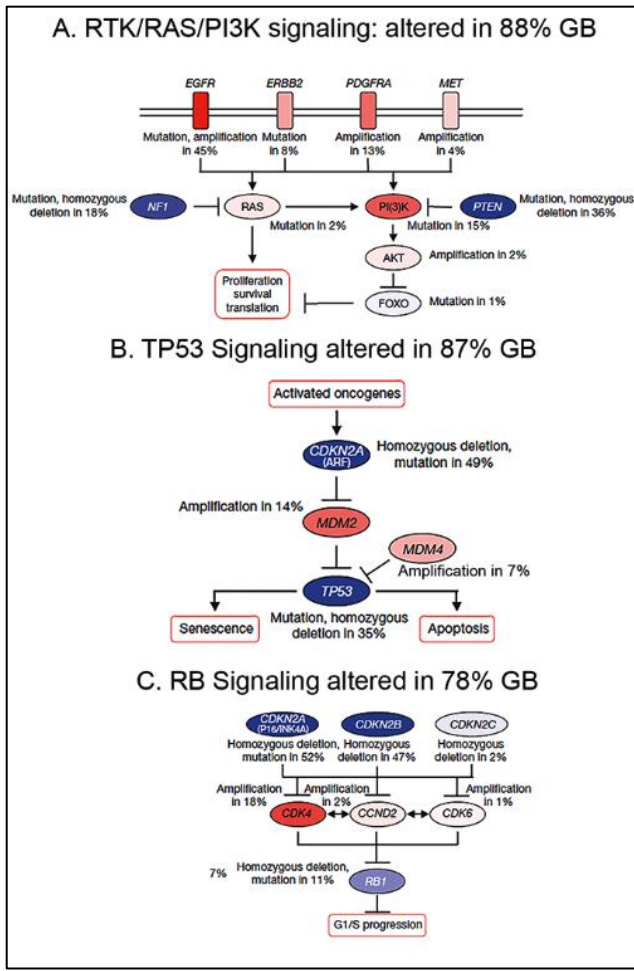
Figure 1 Schematic representation of the three critical signaling pathways with the most common genetic alterations found in glioblastoma: (A) RTK/RAS/PI3K, (B) TP53 and (C) RB. Adapted from The Cancer Genome Atlas Network (Network, 2008).

function represent the most common (40%) genetic alteration in GB (Gan et al., 2009). A mutated, truncated, constitutively active form of EGFR: EGFRvIII is found in 20-30% of GB patients. Presence of this mutated form results in survival advantage and increased proliferation of glioblastoma cells (Heimberger et al., 2005).

The telomerase reverse transcriptase (TERT) is a subunit of the telomerase enzyme that when expressed, allows cells to lengthen their telomeres and avoid senescence. Overexpression of TERT is found in the majority of cancers as well as in stem cells. Mutations in the TERT promoter result in increased expression of the gene and activity of the enzyme and have been identified in 74.2 % of grade IV GB and 79.3% oligodendrogliomas and with lower frequency in grade II-III astrocytomas (18.2%) (Killela et al., 2014).

Isocitrate dehydrogenase (IDH) is a rate limiting enzyme in the Krebs cycle with important roles in regulating metabolism. Mutations in IDH1 have been identified in more than 70% of grade II and III astrocytomas and oligodendrogliomas and grade IV recurrent GB (Parsons et al., 2008; Yan et al., 2009). Mutations in IDH2 are also commonly present in gliomas. Mutations in IDH1 and IDH2 are correlated with increased survival of low grade glioblastoma and recurrence of lower grade gliomas into high grade glioblastoma. IDH catalyzes the production of α-ketoglutarate from isocitrate. If IDH1/2 is mutated, isocitrate is converted

into 2-hydroxy-glutarate, an onco-metabolite that induces expression of hypoxia inducible factor alpha (HIF1α) and of VEGF, factors that induce a glioma stem cell phenotype and promote recurrence (Huang et al., 2019).

Glioma Stem Cells

Stem cells are defined as slow cycling cells that undergo self-renewal for an indefinite period of time and, upon specific induction, are able to generate terminally differentiated cells, either of all phenotypes (totipotent stem cells) or of tissue specific phenotypes, for tissue specific stem cells. Neural Stem Cells (NSCs) can generate all the cells present within the nervous system, including neurons and glia (astrocytes, oligodendrocytes and Schwann cells). Similarly, Glioma Stem Cells (GSCs) represent a small population of slowly dividing cells present within the tumors, that are able to self-renew, give rise to differentiated progeny and to generate tumors upon a secondary transplantation, tumors that recapitulate the cellular heterogeneity and histological appearance of the original tumor (Stiles and Rowitch, 2008). GSCs share many characteristics of NSCs including high proliferative potential, association with blood vessels, telomerase activity, high motility, diversity of progeny and similar gene expression profiles, including Nestin, CD133, Olig2, Sox2, Sox4, Integrin α6, CD15, L1CAM, A2B5, CD44 and others (Singh et al., 2003; Ligon et al., 2007; Bao et al., 2008; Beier et al., 2011; Calinescu et al., 2016).

GSCs are highly resistant to chemo- and radiotherapy and promote neovascularization. Treatment of GB cells with temozolomide, the most commonly used chemotherapeutic in GB, consistently increases the percentage of GSCs over time, with cells expressing higher levels of CD133, SOX2, OCT4 and displaying increased tumor forming ability in experimental mice (Auffinger et al., 2014). CD133+ GSCs isolated from primary cell cultures of human GB showed significant resistance to several chemotherapeutic agents, including temozolomide, carboplatin, paclitaxel and etoposide compared to non-GSC cells (CD133-)(Liu et al., 2006). Following irradiation, the percentage of CD133+ GSCs increased, demonstrating radio-resistance of these cells (Bao et al., 2006a). Irradiation kills cancer cells primarily through DNA damage. It was demonstrated that CD133+ GSCs have increased activation of the DNA damage response proteins ATM, Rad17, Chk1 and Chk2, with subsequent increased DNA damage repair that conferred increased resistance to radiation (Bao et al., 2006a).

Glioblastoma is a highly vascular tumor. Neo-angiogenesis, the formation of new blood vessels within the tumor, is induced in large part by VEGF. Expression of VEGF is in its turn stimulated by hypoxia, through promoter activation by hypoxia inducible factors HIF1α and HIF1β. GSCs express increased levels of VEGF that is further induced by hypoxia and HIF1α is critical to the survival of GSCs and tumor growth (Bao et al., 2006b). HIF1α also induces expression of the CXCL12, a chemokine that localizes in regions of necrosis and proliferating microvessels in GB (Tabatabai et al., 2006; Komatani et al., 2009) as well as in the subventricular zone, a Neural Stem Cell niche in the adult brain (Goffart et al., 2014). CXCL12 has also been demonstrated to mediate resistance to radiation therapy in a mouse model of GB (Goffart et al., 2016).

The role of CXCL12 and its receptor CXCR4 in Glioblastoma

Chemokines are small secreted proteins from a specific class of cytokines that are elevated during inflammation or infection and attract eosinophils, neutrophils, macrophages and other immune cells. Chemokines regulate physiological and pathological cellular processes that can function either in an autocrine or paracrine manner. Chemokines have also well documented roles during development, when they guide the migration of newly formed cells to their final destination. An increasing body of literature documents the role of chemokines in modulating the tumor microenvironment (TME) and their participation in tumor progression. CXCL12 is a chemokine that signals via its cognate receptor CXCR4 and that has been shown to control cell survival, proliferation and migration of tumor cells and promote cancer stem cell maintenance, dissemination, metastasis as well as neo-angiogenesis in numerous hematological and solid cancers (Domanska et al., 2013; Peitzsch et al., 2015).

In the context of GB, enhanced expression of CXCL12 is found in response to hypoxia and irradiation. Expression of CXCL12 was maximally localized to hypoxic regions of pseudopallisading necrosis and proliferating microvessels. High expression of CXCL12 and of its cognate signaling receptor CXCR4 has been correlated with worse prognosis of GB patients (Komatani et al., 2009). High expression of CXCR4 correlated also with increased tumor grade (III, IV) and increased invasiveness of glioblastomas (Stevenson et al., 2008). Increased levels of CXCL12 due to hypoxia and necrosis as well as following irradiation led to recruitment of hematopoietic myeloid cells (Tabatabai et al., 2006; Kioi et al., 2010). These myeloid cells have

immune suppressive properties, inhibiting the native anti-tumor immune response and also constitute the building blocks for the formation of abnormal vascular structures, promoting further tumor growth and invasion (Kioi et al., 2010). High expression of CXCL12 by GSCs also induced VEGF production and tumor angiogenesis (Ping et al., 2011). Inhibition of the CXCL12/CXCR4 signaling axis prevented recurrence and inhibited the growth of intracranial tumors in animal models of GB (Rubin et al., 2003; Kioi et al., 2010). CXCL12 has also been described as the essential factor of inducing resistance to radiotherapy of Glioma Stem Cells (GSCs) (Goffart et al., 2016) as well as a key mediator of continued proliferation of GSCs under hypoxic stress, promoting cell cycle progression and inhibiting apoptosis (Calinescu et al., 2016).

Several clinical trials are currently ongoing, testing the effect of the CXCR4 inhibitor AMD3100 (Plerixafor, Mozobil) as adjuvant agent for the treatment of glioblastoma. A phase I/II clinical trial (ClinicalTrials.gov identifier: NCT01977677) testing the use of AMD3100 over the course of four weeks, starting one week prior to the completion of standard irradiation has been recently completed. The goal was to see if the treatment can reduce re-establishment of tumor vascularization following therapy with temozolomide and irradiation. Results show that the dose of AMD3100 used (16.6 µg/kg/hr) was well tolerated and that, compared to contemporary controls treated with irradiation and temozolomide only, the relative cerebral blood volume was significantly reduced in patients receiving AMD3100 (Thomas et al., 2018). This study has now moved to phase II (NCT03746080). Another phase I and biomarker study (NCT01339039) using AMD3100 in combination with Bevacizumab (Avastin, a monoclonal antibody inhibiting VEGF) in recurrent high grade glioma has recently been concluded. This study established that the doses used for AMD3100 (320µg/kg) and bevacizumab (10mg/kg) were well tolerated. Doses of AMD3100 in the CSF were 26.8 ng/ml and in the resected tumor tissue (10-12 µg/g) and there was a significant increase in the plasma concentration of CXCL12 and placental growth factor. The authors conclude that the treatment was accompanied by good distribution of the drugs in the tissue and biomarker changes consistent with CXCR4 and VEGF inhibition (Lee et al., 2018). These are encouraging studies, warranting further therapeutic exploration of the use of CXCL12/CXCR4 inhibitors for the treatment of glioblastoma.

G-Protein Coupled Receptors

The cognate signaling receptor for CXCL12 is CXCR4, member of the G-protein coupled receptors (GPCR) superfamily. GPCRs are seven-transmembrane (7TM) receptors representing the largest class of membrane receptors, signaling portals for numerous sensory receptors including photoreceptors, olfactory and taste receptors, neurotransmitters, hormones, chemokines and calcium ions. They are called GPCRs as classical signaling through these receptors occurs via coupling to small G proteins. In the absence of ligand agonist, the GPCR is bound to the G protein complex and guanosine diphosphate (GDP). Upon ligand binding, GDP is released and replaced by guanosine triphosphate (GTP), leading to the formation of an activated receptor, dissociation of the G protein complex and release of its subunits: $G\alpha$ and the $G\beta\gamma$ dimer. These subunits then activate downstream signaling cascades, including adenylyl cyclase (AC) resulting in conversion of ATP to cAMP, subsequent activation of Protein Kinase A (PKA) and generation of a specific cellular response (Pierce et al., 2002). Classical GPCR activation also results in calcium mobilization through increased intracellular influx and calcium release from endogenous storage compartments. Activation of GPCRs is quickly terminated, hydrolysis of GTP to GDP results in re-association of the $G\alpha\beta\gamma$ protein heterotrimer and conformational changes of the GPCR to its inactive state. Even in the presence of continuous agonist, signaling through GPCRs is dampened, a phenomenon known as "desensitization". Rapid desensitization can occur through receptor phosphorylation by PKA or PKC or by G-protein-coupled receptor kinases (GRK). Desensitization also occurs through internalization of the receptors, process coordinated by the binding of β-arrestin molecules to the activated GPCR. The process of internalization has also been proposed to serve as a re-sensitization mechanism and to positively regulate receptor signaling, a process dependent on the presence of β-arrestin (Ferguson, 2001). A schematic of the GPCR de-sensitizing steps is presented in **Figure 2** (adapted from (Luttrell, 2008)).

Signaling through the CXCL12/CXCR4 axis occurs via the classical GPCR pathway. CXCR4 is bound by the heterotrimeric G-protein complex consisting of the α,β,γ subunits. The $G\alpha$ complex consists of four subunits $G\alpha_s$, $G\alpha_i$, $G\alpha_q$ and $G\alpha_{12}$. $G\alpha_s$ stimulates AC whereas $G\alpha_i$ inhibits it. $G\alpha_q$ activates Phospholipase C (PLC) resulting in generation of inositol triphosphate (IP3) and Diacylglycerol (DAG), which increases the intracellular concentrations of Ca_{++} and activates the NF-kB pathway (Peitzsch et al., 2015).
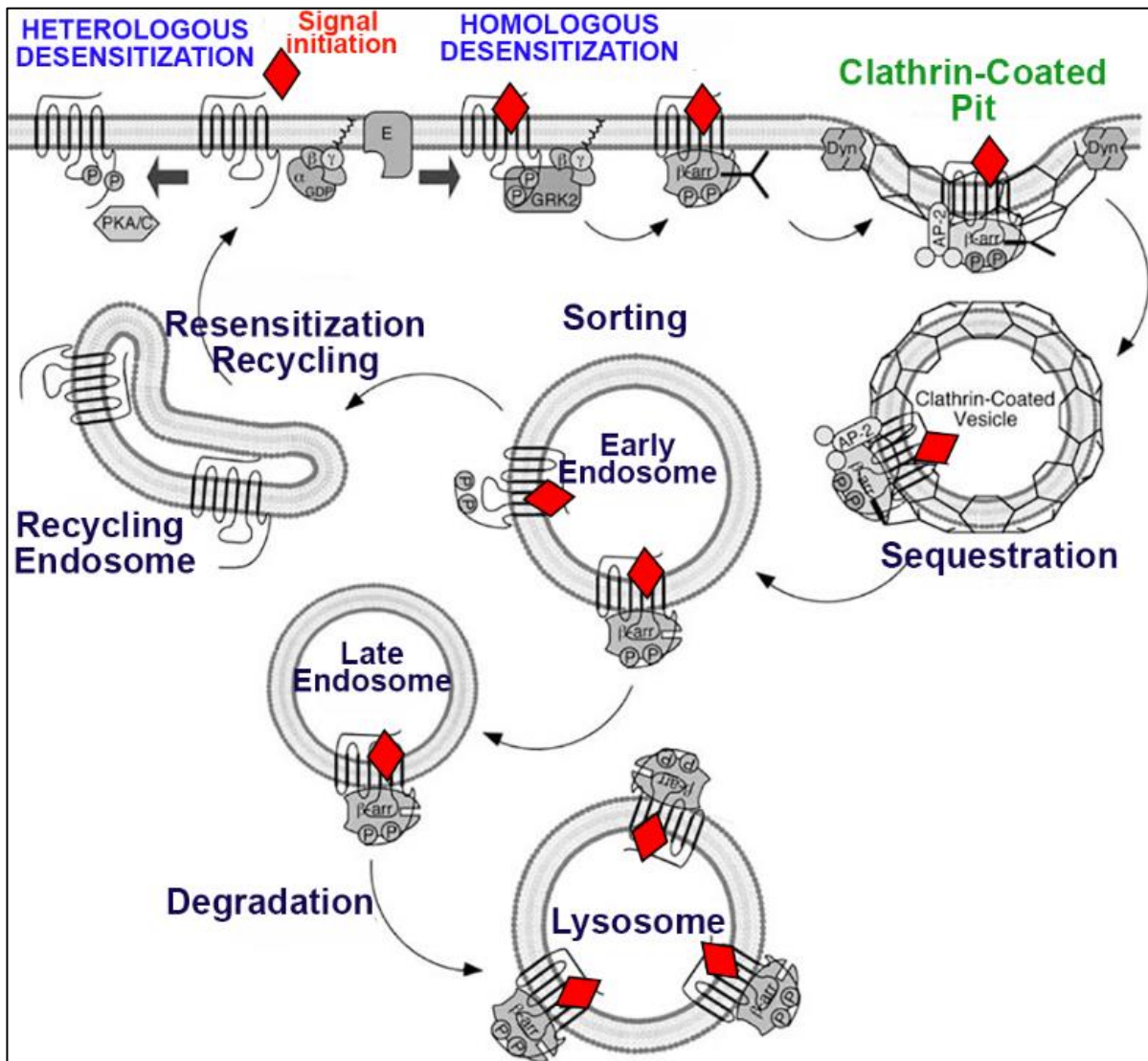
Figure 2 Schematic representation of the desensitization, sequestration and recycling of GPCRs. Ligand binding induces phosphorylation of GPCRs by either PKA/PKC or by, GRK. PKA/PKC phosphorylation leads to heterologous desensitization whereas GRK phosphorylation leads to □-arrestin binding and homologous desensitization. This is followed by endocytosis within clathrin-coated vesicles and endosomal sorting to either re-sensitization and recycling or lysosomal degradation. (Adapted from "Transmembrane Signaling by G Protein-Coupled Receptors (Luttrell, 2008).

Both Gα_i and Gα_q activate the PI3K and the MAPK pathways, resulting in alterations in gene expression, cell structure rearrangements and migration (Peitzsch et al., 2015). Thus, this interaction between CXCL12 and CXCR4 can lead to many downstream events which can affect intracellular Ca$_{2+}$ concentration, cell survival/proliferation, cell migration, chemotaxis, and gene expression (Hattermann and Mentlein, 2013; Peitzsch et al., 2015).

Desensitization of the CXCR4 receptor occurs through phosphorylation by GRK at serine sites located on the C terminal end of the receptor, followed by recruitment of β-arrestin, clathrin-coated pit internalization and endosomal sorting for ubiquitin dependent degradation (Peitzsch et al., 2015) and the references within)). When CXCR4 is bound by β-arrestin it is decoupled from Gα_i signaling resulting in β-arrestin mediated MAPK activation. (Peitzsch et al., 2015). After the internalization of the receptor, CXCR4 can either undergo re-sensitization or ubiquitin-dependent degradation. Re-sensitization can be initiated simply through de-phosphorylation of the serines on the intracellular C-terminus; this allows CXCR4 to shuttle back to the plasma membrane and allow CXCL12 to bind again (Luttrell, 2008).

CXCL12 represents the only ligand for CXCR4. Nonetheless, CXCL12 binds with 10 fold higher affinity to another GPCR, namely CXCR7, receptor that has two ligands: CXCL12 and CXCL11 (Balabanian et al., 2005).

CXCR7 Discovery and Signaling

The gene encoding the CXCR7 receptor is located in close proximity to the genes encoding other chemokine receptors (CXCR1, CXCR2, CXCR5) on chromosome 2 in humans and chromosome 1 in mice. Given its sequence and structural similarity with other chemokine receptors, widely expressed by immune cells, Balabanian et al. tested whether CXCR7 is expressed on white blood cells, using immunohistochemistry, and discovered that it was (Balabanian et al., 2005). Interestingly, the authors found that antibody staining was inhibited by the addition of CXCL12, similar to staining of CXCR4. They also discovered that the chemotactic effect induced on lymphocytes by CXCL12 was inhibited by antibodies against CXCR7, as it was by antibodies against CXCR4. A new receptor for CXCL12 was thus found.

Mice deficient in *Cxcr7* are perinatal lethal, due to defects in heart development involving the ventricular septum and semilunar heart valves. The same phenotype is found in mice in which the Cxcr7 is absent from only endothelial cells, suggesting a critical role of this

receptor in endothelial cell growth and survival (Sierro et al., 2007). It was also established that in addition to CXCL12, another chemokine activates CXCR7, as CXCL12 deficient mice do not show the heart valve anomalies. Upon testing of a panel of chemokines, CXCL11 was identified as the alternate ligand for CXCR7 (Sierro et al., 2007). Expression of CXCR7 was found on many tumor cell lines and a role in tumor cell growth and survival was established using *in vitro* assays as well as *in vivo* experiments in mice with subcutaneous implantations of lung carcinoma and lymphoma cell lines. Tumor cell growth was inhibited by a specific small molecule inhibitor of CXCR7 (CCX771, Chemocentrix) (Burns et al., 2006).

Unlike other GPCRs, activation of CXCR7 did not result in $G\alpha_i$ -protein dependent signaling and did not mobilize intracellular calcium in response to CXCL12; instead, it appeared to form heterodimers with CXCR4 in HEK-293T cells (Human Embryonic Kidney cells) overexpressing both receptors and to inhibit the calcium mobilization through CXCR4 (Levoye et al., 2009). Soon thereafter it was demonstrated that CXCR7 acts as a specific scavenger of CXCL12, inducing ligand internalization and targeting the bound chemokine for degradation, reducing the level of CXCL12 from the surrounding environment. This internalization does not require coupling to G-proteins and it is dependent on the C-terminal end of the receptor (Naumann et al., 2010). The authors also demonstrated that CXCR7 shuttles continuously between the intracellular and membrane compartment, irrespective of the presence of the ligand, in both mammalian cells and zebrafish embryos, making CXCR7 an almost constant presence on the cell surface. When CXCL12 binds to CXCR4, the receptor typically undergoes internalization or sequestration in order to desensitize the receptor. Thus, CXCL12 stimulates concentration-dependent sequestration of CXCR4 from the plasma membrane. Approximately 50% of CXCR4 receptors were sequestered after twenty minutes of CXCL12 and only 10-25% of CXCR7s were sequestered following sixty minutes (Naumann et al., 2010).

CXCR7 is therefore defined as an "atypical" or "decoy" chemokine receptor, that binds CXCL12 and CXCL11 with high affinity, but fails to couple with G-proteins and induce typical GPCR responses. In the same category fall DARC, Duffy, D6 and others, that are considered non-signaling receptors that scavenge and modulate the availability of chemokines, and thus modulate numerous physiological and pathological processes (Ulvmar et al., 2011).

Nonetheless, it has been shown that ligand binding to CXCR7 can activate signaling pathways through its recruitment of β-arrestin, process that results in activation of the MAPK

pathway, as evidenced by increased phosphorylation of ERK and increased migration of the vascular smooth muscle cells in response to CXCL12 and CXCL11 (Rajagopal et al., 2010). Activation of CXCR7 also led to β-arrestin mediated activation of Akt in primary CD34+ hematopoietic stem and precursor cells (HSPCs) and induced increased expression of Cyclin D1, D3, E1 and reduced expression of the cyclin dependent kinase inhibitor p27 in HSPCs, effect that was dependent also on the presence of the CXCR4 receptors (Torossian et al., 2014).

Findings from these studies converge to generate a complex and interconnected landscape of signaling mechanisms and pathways induced by CXCL12. CXCR4, through classical G-protein signaling activates the PI3K/Akt, IP3 and MAPK pathways to induce cell survival, proliferation, chemotaxis and migration. Binding of CXCL12 to CXCR7 results in recruitment of β-arrestin, receptor internalization and scavenging of the extracellular CXCL12. Activation of CXCR7 can also induce MAPK and Akt activation, migration and cell cycle progression. Less understood are signaling mechanisms through CXCR4/CXCR7 heterodimers. A schematic representation of these pathways is presented in **Figure 3.**
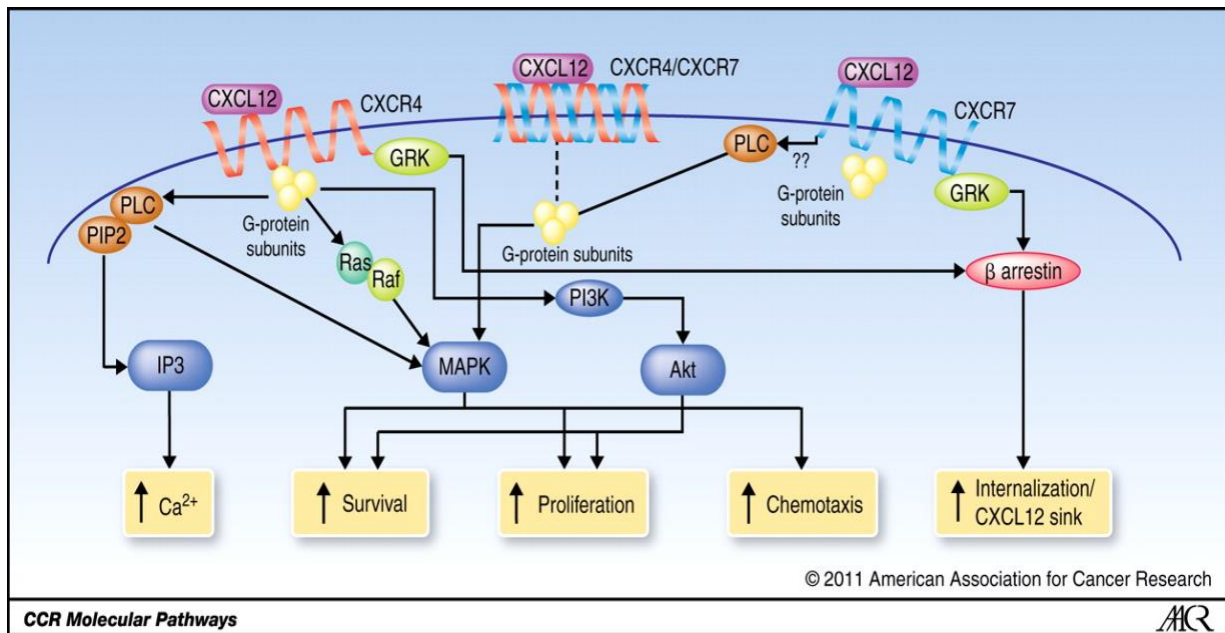
Figure 3. Schematic representation of signaling pathways activated by CXCL12. Binding of CXCL12 to CXCR4 results in classical GPCR signaling through G-protein subunits, leading to Calcium influx, Ras/Raf/MAPK and PI3K/Akt pathway activation resulting in increased survival, proliferation and chemotaxis. Binding of CXCL12 to CXCR7 leads to β-arrestin recruitment, internalization of the receptor and decrease of CXCL12 in the extracellular environment. CXCR7 activation can also trigger MAPK activation through β-arrestin recruitment. CXCR4/CXCR7 heterodimers are also activated by CXCL12, process that results also in activation of the MAPK pathway. (Adapted from (Duda et al., 2011)

CXCR7 and Cancer

Soon after it was discovered that CXCR7 is a GPCR that binds CXCL12, a role for CXCR7 in tumor growth and progression has been described. It was reported that CXCR7 is highly expressed on several tumor cell lines (lung carcinoma, breast cancer and lymphoma) and that inhibition of CXCR7 with a specific small molecule inhibitor decreased the growth of tumor cells (Burns et al., 2006). Since then, numerous studies have described a role for CXCR7 in a variety of cancers including breast, lung, cervical, pancreatic, myeloid, lymphomas, head and neck cancer, glial and prostate carcinoma [(Sánchez-Martín et al., 2013; Freitas et al., 2014) and the references within], arguing that expression of CXCR7 is a negative prognostic marker and promotes cancer progression and metastasis. CXCR7 is primarily localized to activated endothelial cells in the tumors and it was shown to promote angiogenesis in prostate carcinoma (Wang et al., 2008) as well as in hepatocarcinoma (Zheng et al., 2010). Expression of high levels of CXCR7 has been proposed to represent an identifying marker for tumor vasculature (Freitas et al., 2014).

In patients with lung cancer, high levels of TGFβ1 often correlate with poor prognosis, angiogenesis and tumor progression. High levels of TGFβ1 also promote the cancer stem cell phenotype in lung carcinoma cells, as well as epithelial to mesenchymal transformation (EMT), phenotypic shift characteristic of metastatic cells (Wu et al., 2016). It was demonstrated that TGFβ1 also induced expression of CXCR4 and CXCR7. Knockdown of CXCR7, but not of CXCR4, inhibited TGFβ1-induced migration, EMT and cancer stem cell phenotype, as evidenced by reduced expression of Nanog, Sox-2, and Oct-4 (Wu et al., 2016). This suggests that CXCR7 is a key receptor for TGFβ1 induced progression of lung cancer and that the CXCL12/CXCR7 axis plays an important role in migration, EMT and cancer stem cell phenotype in lung cancer.

The CXCL12/CXCR7 axis also plays an important role in the invasive phenotype of pancreatic cancer (Guo et al., 2016). When CXCR7 was silenced, migration and invasion decreased and the opposite was observed when CXCR7 is overexpressed (Guo et al., 2016). Likewise, CXCL12 also promoted invasion, proliferation and chemoresistance through interaction with CXCR4 in pancreatic cancer. Patients with high expression of both CXCL12 and CXCR7 had the poorest prognosis (Guo et al., 2016). Mechanistically, it was found that the CXCL12/CXCR7 axis directly influenced the phosphorylation of various components in the

mTOR signaling pathway, which further activated Rho/ROCK pathway and promoted tumor cell migration and invasion (Guo et al., 2016).

A study using overexpression and RNA interference to modulate expression of CXCR7 in breast and lung tumor cells and *in vitro* and *in vivo* analysis of tumor growth showed that CXCR7 promoted tumor growth, independently of CXCR4, and promoted angiogenesis, demonstrating a key role for CXCR7 in tumor progression (Miao et al., 2007). This study also demonstrated high expression of CXCR7 in tumors from patients with breast and lung carcinoma, and its absence from normal tissue. It has also been reported that CXCR7 promoted breast tumor metastasis and angiogenesis and that blocking CXCR7 with the small molecule inhibitor CCX771 reduced breast tumor invasion, adhesion and metastasis (Qian et al., 2018).

In stark contrast to these findings, a study using conditional genetic ablation of CXCR7 on vascular endothelial cells and two different syngeneic orthotopic mouse models of breast cancer, demonstrated that in the absence of vascular CXCR7 there was a significantly greater recurrence of cancer following resection, accompanied by elevated number of circulating tumor cells and more spontaneous metastases, suggesting a protective role of CXCR7 in preventing metastatic spread of breast cancer cells (Stacer et al., 2016). Survival of tumor bearing mice was also significantly decreased in the absence of CXCR7. Consistent with a scavenging role for CXCR7, plasma levels of CXCL12 were elevated in these mice, both in naïve mice as well as in tumor mice. There was a 35% increase in levels of CXCL12 in the extracellular space, which is consistent with the 14% increase in patients with breast cancer, in which progressive increase in CXCL12 correlated with poor prognosis (Stacer et al., 2016). Overall, these results suggest that CXCR7 on vascular endothelium may play an important role in suppressing the progression of breast cancer to a metastatic disease. Notably, this study highlights the importance of analyzing the role of CXCR7 in a cell and tissue specific context and cautions against generalizing conclusions from one study to the next.

CXCR7 in Glioblastoma

The role of the CXCL12/CXCR4 signaling axis in promoting glioblastoma (GB) is firmly established and extensively studied. Inhibitors of CXCR4 are currently used in ongoing clinical trials as adjuvant agents for GB treatment. In contrast, fewer studies exist that analyze the role of CXCR7 in GB. Given the heterogeneity of the disease and the diversity of the different

established and newly generated GB cell lines and patient derived samples, expression studies show either high or low expression of CXCR7 relative to CXCR4 in astrocytomas, primary and recurrent GB (Hattermann et al., 2010; FLüH et al., 2016). Several studies agree that CXCR4 is highly expressed in glioma stem cells (Ping et al., 2011; Würth et al., 2014; FLüH et al., 2016) and that CXCR7 is primarily expressed in more differentiated GB cells (Hattermann et al., 2010; FLüH et al., 2016). It was reported that CXCR7 showed decreased expression in recurrent GB (FLüH et al., 2016). CXCR7 expression increased following differentiation of GSCs, whereas the opposite was found for CXCR4 (Hattermann et al., 2010). In contrast, authors from the Chemocentrix company that produce small molecule inhibitors targeting CXCR7 reported, based on neurosphere formation ability, that expression of CXCR7 promoted the GSC phenotype and CXCR7 blockade inhibited sphere formation (Walters et al., 2014).

A role for CXCR7 in inducing resistance to chemotherapy has also been described (Hattermann et al., 2010). The authors described high expression of CXCR7 in astrocytoma (grades I, II, III) and GB primary cell lines, and activation of the MAPK and PI3K pathways upon treatment with CXCL12. CXCL12 failed to promote migration or proliferation in these cells, instead induced resistance to the chemotherapeutics camptothecin and temozolomide, as indicated by a decrease in apoptosis following drug treatment. Addition of a small molecule inhibitor of CXCR7 (CCX733) restored the apoptosis induced by chemotherapy, suggesting that CXCR7 mediates CXCL12-induced resistance to chemotherapy (Hattermann et al., 2010).

Increased migration of GB cell lines upon CXCR7 activation by CXCL12 has been reported in another study that observed this response only under hypoxic conditions (Esencay et al., 2013). This phenomenon was inhibited by shRNA knock-down of CXCR7 and was absent under normoxic conditions. In this study, inhibiting CXCR4 did not reduce migration towards CXCL12 nor impact the phosphorylation of ERK 1/2 and Akt (Esencay et al., 2013). There are however numerous studies demonstrating the involvement of the CXCL12/CXCR4 signaling axis under hypoxic conditions in GB invasion and progression (Tabatabai et al., 2006; Zagzag et al., 2006; Kioi et al., 2010; Calinescu et al., 2016).

Inhibition of CXCR7 led to increased survival of tumor bearing animals in rat and mouse models of GB following treatment with ionizing radiation (Walters et al., 2014). For patients with GB, radiotherapy is part of the standard of care to reduce tumor size. However, following irradiation, there is high rate of recurrence. Revascularization of the tumor bed following

irradiation is considered a major contributing factor to the relapse. Using specimens from GB patients, Walters et al. show that CXCR7 is expressed in human GB in both tumor cells and vascular endothelial cells, and that higher levels of expression correlate with increased tumor grade. The authors used three different preclinical GB models to test the effect of CXCR7 inhibitors on tumor growth following irradiation: (1) intracranial implantations of a commonly used GB cell line U251 in immunocompromised mice, irradiation with 12 Gy, followed by a three-week administration of the CXCR7 inhibitor CCX771, (2) intracranial implantation of an aggressive syngeneic GB cell line (C6) into rats, irradiation with 18 Gy, followed by 14 days administration of the CXCR7 inhibitor CCX662 and (3) a rat model of GB, where tumors are induced in embryonic rats (E18) with an injection of N-ethyl N-nitrosourea (ENU) into pregnant dams, irradiation of the progeny at postnatal day 115 with 18 Gy, followed by 4 week administration of CCX662. The CXCR7 inhibitors increased survival in irradiated mice in the two rat models and decreased tumor size in the mouse model, but had no effect on animal survival in the absence of irradiation. Interestingly, CCX662 increased survival of rats bearing C6 tumors, that showed very limited expression of CXCR7, localized only in the tumor vasculature. The authors also reported that neurosphere formation was increased in CXCR7+ cells isolated by flowcytometry from patient derived xenografts, when compared to CXCR7- cells. Inhibition of CXCR7 with CCX771 impaired neurosphere formation. The authors conclude that recurrence of GB following irradiation is a phenomenon dependent on CXCR7 that promotes neovascular formation and/or proliferation and survival of glioma stem cells and propose that inhibition of CXCR7 following irradiation as a promising treatment approach to improve patient outcome (Walters et al., 2014). What is missing from this interesting study is the post-treatment analysis of the tumors to ascertain for example the distribution and density of tumor vasculature, as well as the frequency of GSCs in the tumor tissue, in order to substantiate the process that lead to the increased survival of the tumor bearing animals and the *in vivo* mechanism of action of the two CXCR7 inhibitors used.

Statements and Goals for the Thesis

Taken together, all these studies confirm the well-established role of the CXCL12 chemokine in promoting GB pathogenesis and progression, effects largely attributed to the activation of CXCR4, and classical G-protein mediated signaling pathways. In contrast, studies of the role of CXCR7 in various cancers, including GB, present conflicting results. CXCR7 appears to either promote or inhibit cancer progression, promote or inhibit metastasis, promote or inhibit the cancer stem cell phenotype. This wide range of experimental results may be related to the complexity of CXCL12 signaling through the two receptors, its ability to bind to both CXCR4, CXCR7 as well as to CXCR4/CXCR7 heterodimers and likely more than anything to the larger context of details in the cellular makeup and tumor micro-environmental conditions.

Considering that CXCL12 promotes tumor progression and GSC phenotype and CXCR7 acts as a scavenger receptor for CXCL12, one would expect that the presence of CXCR7 would prevent tumor growth, invasion and recurrence following treatment. Published GB studies seem to indicate that CXCR7 promotes malignancy and recurrence, yet mechanistic details have so far not been conclusively established.

The study herein was designed to systematically address the role of CXCR7 in the progression of GB using *in vitro* and *in vivo* experiments of glioblastoma stem cell growth and activation in the presence of specific inhibitors of CXCR4 and CXCR7 when CXCR7 is overexpressed. Experiments described herein were planned to increase our understanding of the role of CXCR7 in glioblastoma stem cell biology and provide mechanistic insight for the development of new therapies that target the microenvironment of GB to improve survival of patients with GB.

Methods

Subcloning CXCR7 into the lentiviral vector pLentilox-IRES-GFP (pLL-IRES GFP).

To generate CXCR7 expressing cells a lentiviral plasmid encoding CXCR7 was first constructed. A CXCR7 expression plasmid (pEGFP-CXCR7) gift from Drs. Kathy and Gary Luker (Luker et al., 2009) was used as source for the human CXCR7 open reading frame (ORF) and the lentiviral vector pLL-IRES GFP as receiving vector. A schematic of the cloning strategy is presented in **Supplementary Fig.1**. In brief, to release the CXCR7 ORF, the pEGFP-CXCR7 plasmid was first digested using the restriction enzymes NheI and AgeI. The vector was linearized with XbaI. The restriction digest reactions were resolved by agarose gel electrophoresis (**Supplementary Fig. 2**). The insert and vector DNA fragments were cut from the gel, column purified and the resulting DNA quantified with a spectrophotometer. Since the ends of the vector and insert were incompatible for ligation, their ends were blunted using the Quick Blunting kit. Subsequently, the vector was dephosphorylated to prevent self-assembly. DNA fragments were column purified and concentration of the DNA measured again. Ligation reactions with T4 DNA ligase were setup according to the manufacturer's protocol. Ligations with two different ratios of vector to insert (3:1 and 7:1) were setup using 50ng of vector and appropriate femtomolar ratios of the insert, calculated using the New England Biolabs Inc. ligation calculator tool. The reaction was run overnight at 16_oC in a thermocycler. A control reaction was included with vector only, without insert. The following day, ligation reactions were transformed into NEB® Turbo Competent high efficiency chemically competent E. coli cells. Transformed bacteria were cultured onto ampicillin resistant LB-agar plates. Colonies were selected from the plates and PCR reactions were assembled with specific primers for the insert (HCXCR7 F1) and vector (EGFP R1). The size of the expected amplification product was 2388 base pairs. PCR reactions were resolved on an agarose gel. Results show that three colonies in the 3:1 ligation and 1 colony in the 7:1 ligation have amplification products in the range of the expected size (**Supplementary Fig. 2**). DNA was extracted from the cultures from the colonies 2,7,8,17 and a restriction digest was performed with NotI and NheI to release the CXCR7 fragment, to determine if it was incorporated into the vector. Results indicate that colonies 2, 7, and 8 had the expected plasmid, whereas colony 17 did not (**Supplementary Figure 4**).

To conclusively confirm the sequence identity of the newly generated plasmid, DNA from colonies 2, 7, and 8 was sent to the University of Michigan DNA Sequencing Core for

Sanger Sequencing. Sequencing results were compared to the predicted reconstituted sequence of pLL-CXCR7-IRES-GFP using the SeqBuilder Pro tool of the DNASTAR LASERGENE Software package and the blastn suite from the National Center for Biotechnology Information (NCBI). Since the automated sequencing can only produce 1000 nucleotides of sequence and our ligated plasmid is 8960 bp, several comparisons were made, and it was found that there was around 97-99% accuracy between the ligated vector from lanes 2, 7, 8 and the reconstituted vector. The 1-3% that did not match were likely because of the unreliability at the beginning and end of the sequence product during Sanger Sequencing. The reconstituted CXCR7-GFP sequence is presented in the **Supplementary Figure 5A,** this sequence was correct in the DNA from colonies 2,7 and 8, confirming that the ligation was successful and we generated a lentiviral vector that encodes the human CXCR7 gene.

Generation of Glioblastoma Stem Cells.

All animal experiments were done in concordance with standards of humane and responsible use of animals and approved by the Institutional Animal Care and Use Committee of the University of Michigan under the protocol PRO0008346 "Engineering stem cells as diagnostic and therapeutic agents for glioblastoma", Principal Investigator- Alexandra Calinescu.

Glioblastoma Stem Cells were generated as described (Calinescu et al., 2015) using the Sleeping Beauty transposase system to transform Neural Stem Cells in the Subventricular Zone of postnatal day 1 mouse pups (C57BL/6J, 000664 Jackson Laboratories) with oncogenes. The following oncogenes were used: NRAS-G12V (an activated mutated form of NRAS that leads to accumulation of GTP bound NRAS and increased downstream pathway activation), henceforth referred to as NRAS, SV-40 Large T antigen (referred to as LgT) and a short hairpin targeting the tumor suppressor TP53, referred to as shp53. In brief, plasmids encoding either NRAS and LgT or NRAS and shp53 as well as a plasmid encoding the Sleeping Beauty transposase and luciferase, were injected into the lateral ventricle of postnatal day 1 (P1) mouse embryos. Previous experiments have demonstrated that these combinations of oncogenes induce tumors that display histological and immuno-histochemical features of human glioblastoma, including pseudopallisading necrosis, invasive phenotype, abnormal glomeruloid vasculature as well as regions of hemorrhage (Calinescu et al., 2015; Calinescu et al., 2016). Mice were allowed to grow to adulthood. Tumor formation was monitored with bioluminescence. Animals were

euthanized when bioluminescence reached a threshold between 5×10^6-5×10^7 photons/sec/cm2/sr. Tumors were dissected, dissociated into single cell suspension using a non-enzymatic dissociation reagent (Accutase) and GSCs were cultured in serum-free Neural Stem Cell culture medium, referred to from here on as NSC medium (DMEM/F12 with Penicillin and Streptomycin (100 U/ml) supplemented with B27, N2, and 20ng/ml of Epidermal Growth Factor (EGF) and basic Fibroblast Growth Factor (bFGF). Neurospheres were allowed to grow for 4-5 days, collected by centrifugation, dissociated with Accutase, expanded in culture, used for experimental analysis or frozen in liquid nitrogen for long term storage. The following GSC lines were used in the experiments presented in this study: GSC1, GSC4, GSC5, transformed with NRAS and LgT and NP3 and NP33, transformed with NRAS and shp53.

Lentiviral transduction of Glioma Stem Cells

Lentiviral particles were generated at the University of Michigan Vector Core using the CXCR7 expressing lentiviral vector: pLL-CXCR7-IRES-GFP. GSCs were collected by centrifugation, dissociated with Accutase, counted and plated onto 6-well tissue culture plates at a density of 1×10^6 cells/ml/well, in serum-free NSC medium. Three hours later, 300 microliters of a 10x concentrate of viral particles and 2 microliters of the linker molecule Polybrene 10 mg/ml were added to each well. Cells were incubated for 24h in a humidified incubator at $37_\circ C$ with 5% CO_2 enriched air. After 24h, fresh medium was added to the well. Transduction efficiency was verified by fluorescent microscopy 72h later.

Quantitative Real Time PCR

RNA was extracted from GSCs and quantified using a spectrophotometer. Equal amounts of RNA (500ng-2μg) were used to generate the complementary DNA that was used as template for the quantitative RT-PCR reactions, performed in triplicate for each template and specific primer pair. QPCR reactions were run on the BioRad CFX Connect Real-Time PCR Detection System. The primer sequences are presented in the Supplementary Table 2. Data was analyzed according to the Delta/Delta Ct method (Pfaffl, 2001). Graphical representation and statistical analysis (Student t-test) was performed with the GraphPad Prism 7.00 software.

Growth dynamics and viability assays of GSCs in culture.

For the analysis of growth and viability of GSCs treated with the CXCR4 (AMD3100) and CXCR7 inhibitors (CCX771), GSCs were dissociated and plated at a concentration of 3000 or 5000 cells/well in 200 microliters of NSC medium/well onto 96 well white, opaque plates, in quadruplicate wells per conditions. In some experiments, inhibitors were added at the concentrations specified for each experiment presented. Cells were allowed to grow for up to six days (144 h). At specified timepoints, cell viability and growth was analyzed with a multimodal plate reader (ID3, Molecular Devices) using the Cell Titer-Glo® Luminescent Cell Viability Assay (Promega), according to the manufacturer's recommendation. Graphical representation of results, nonlinear regression goodness of fit (R_2) and calculation of the half-maximal inhibitory concentration IC_{50} for each drug as well as statistical analysis (Student t-test) were done using the GraphPad Prism 7.00 software.

Orthotopic implantation of GSCs into the striatum of mice and tumor size analysis.

GSCs were cultured in NSC medium, dissociated and counted and a suspension of 25,000 cells/microliter sterile saline was prepared. Two microliters of this suspension, a total of 50,000 cells (GSC4 and GSC4X7), were injected into the striatum of Rag1 knock-out mice (002216 B6.129S7-RAG1tm1Mom/J, Jackson Laboratories) as described (Calinescu et al., 2016). In brief, animals were anesthetized with isoflurane, the fur on the scalp was trimmed, animals were secured in a stereotaxic frame, analgesics were administered subcutaneously, and eyes were protected by lubrication. Three rounds of alternating sterile scrubs with betadine and sterile saline were administered on the scalp and a small midline incision of about 1.5 cm was made. The skin was pulled apart and a small hole was drilled in the skull, 0.5mm anterior and 2mm lateral to the bregma. A 10 microliter Hamilton syringe equipped with a 30-gauge needle was filled with the cell suspension, secured in an automatic injector (UMP3, World Precision Instruments) and was slowly lowered into the skull through the burr hole to a dorso-ventral depth of 3.5 mm and then slowly retracted for 0.5mm. This created a small pocket where the cells were delivered, by slow injection of the 2 microliters of cell suspension over the course of 2 minutes. After another 2-minute wait, the needle was slowly retracted, one millimeter per minute, to prevent reflux of cells to the surface. The skin was sutured with 3-4 interrupted stitches, 0.5 ml of warmed saline was injected subcutaneously to aid the warming, hydration and rapid recovery

of the mouse and the mouse was placed under the heating lamp, where it recovered within 2-5 minutes. Animals were closely monitored daily for the following week. To determine the sizes of the tumors that were formed, two weeks after intracranial implantations animals were anesthetized and intra-cardially perfused, first with saline and then with fixative (4% paraformaldehyde in phosphate buffered saline (PBS)) to preserve the histological integrity of the brain. Brains were carefully removed from the skull using a small rongeur, post-fixed in 4% paraformaldehyde for another 24h, cryopreserved with a 20% solution of sucrose PBS for the next 24-48h, embedded in cryo-sectioning medium, frozen in a dry ice/ethanol slurry and stored in a -80oC freezer until sectioning. Brains were then sectioned in a coronal plane at a thickness of 14 microns and mounted onto negatively charged glass slides. Serial sections were collected, three-four sections per slide in series of 7-9 slides to cover the entire tumor volume. After drying, 1-2 slides from every series were selected for staining. Sections were briefly permeabilized with a solution of PBS and 0.05% Triton X detergent and then stained with the nuclear stain: 4′,6-diamidino-2-phenylindole (DAPI, 1 microgram/ml) for 10 minutes. Slides were washed twice in PBS, cleared in de-ionized water, covered with a water-based mounting medium (FluoroGel, Electron Microscopy Science) and placed horizontally to cure for 24-48h.

Slides were analyzed with an epifluorescent microscope (Olympus IX73 equipped with a DP74 camera and Cell Sens software). The slides with the maximum diameter of the tumor were selected for quantification for each brain. Using the 10x objective composite stitched images were generated to cover the entire coronal sections, scale bars were included on each micrograph. The contour of the tumor, including tumor regions outside of the main tumor area were traced with a digital tablet (Wacom Intuos) and tumor area was calculated in ImageJ by calibrating the image size based on the size of the scale bar. Graphical representation of the resulting areas (in mm2) and statistical analysis (Student t-test) were done using the GraphPad Prism 7.00 software.

Results

Validated expression of CXCR7 in transduced GSCs

To test the role of CXCR7 in the promoting GSC growth and viability we first transduced GSCs with a lentivirus encoding a bicistronic transcript under the control of the cytomegalovirus (CMV) promoter, expressing both the human CXCR7 and Green Fluorescent Protein (GFP) as reporter. To verify the stable integration of CXCR7 and GFP into the genome of GSCs, cells were monitored over multiple passages with a fluorescent microscope, evidencing the
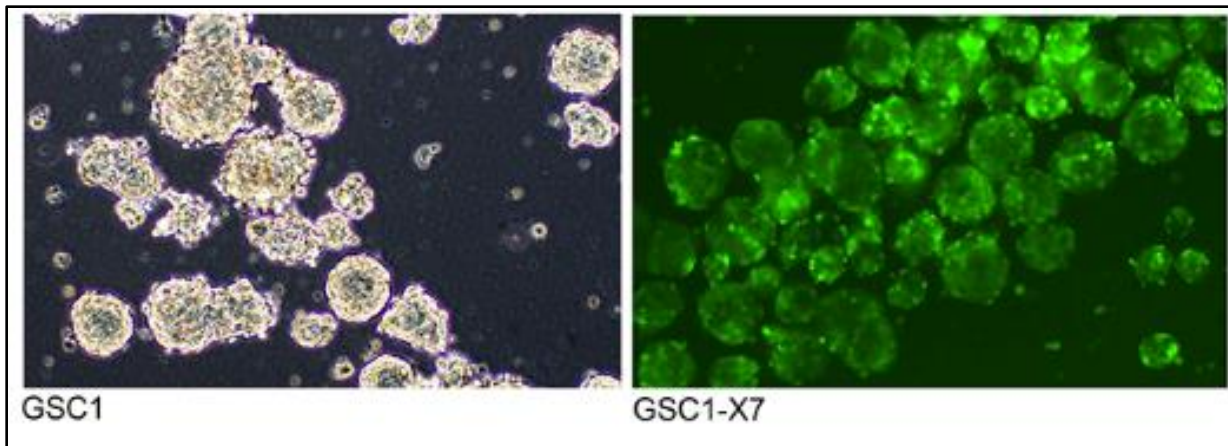
Figure 4 Micrographs of GSC1 and GSC1-X7 illustrating GFP expression in GSCs transduced with the CXCR7 lentiviral particles.

fluorescence of the GFP reporter. A representative micrograph is presented in **Figure 4**, demonstrated that virtually all GSCs transduced with the CXCR7 lentivirus expressed the Green Fluorescent Protein (GFP).

To further validate expression of CXCR7 in multiple transduced GSCs, expression of the human CXCR7 was analyzed in RNA extracted from 5 different transduced GSC lines and their parental counterparts, using quantitative real time reverse transcriptase PCR (QPCR) with specific primers for the human CXCR7. Expression of the mouse hypoxanthine-guanine phosphoribosyl transferase (*Hprt*) was used as control. Expression of CXCR7, normalized to *Hprt*, was then compared to the expression in the non-transduced parental cell line and presented

Cell line	GSC1	GSC1-X7	GSC	GSC4-X7	GSC5	GSC5-X7	NP3	NP3-X7	NP33	NP33-X7
Fold Change CXCR7/HPRT relative to parental line	1	886	1	442	1	1030	1	13,100	1	46,200

Table 1. Expression of the CXCR7 receptor in transduced GSCs, represented as relative fold change compared to the non-transduced parental line.

in the **Table 1** as fold change. Results illustrated increased expression of CXCR7 with a variable fold change ranging from 886-46,200.

To verify that the amplification products of the PCR reaction were of expected size (140 bp), one reaction per cell line and primer pair was resolved on an agarose gel, confirming the specificity of the CXCR7 product (**Figure 4**).
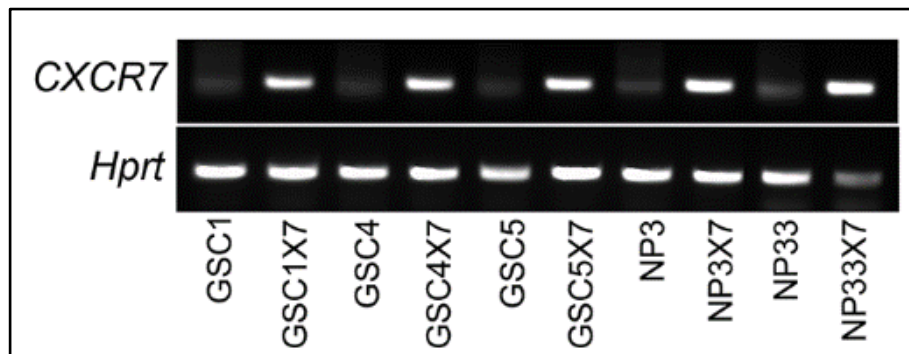
Figure 5. Agarose gel electrophoresis of PCR reactions validating amplification of the human CXCR7 fragment (140bp) in transduced GSCs. The bands of the mouse *Hprt* control gene are presented as control.
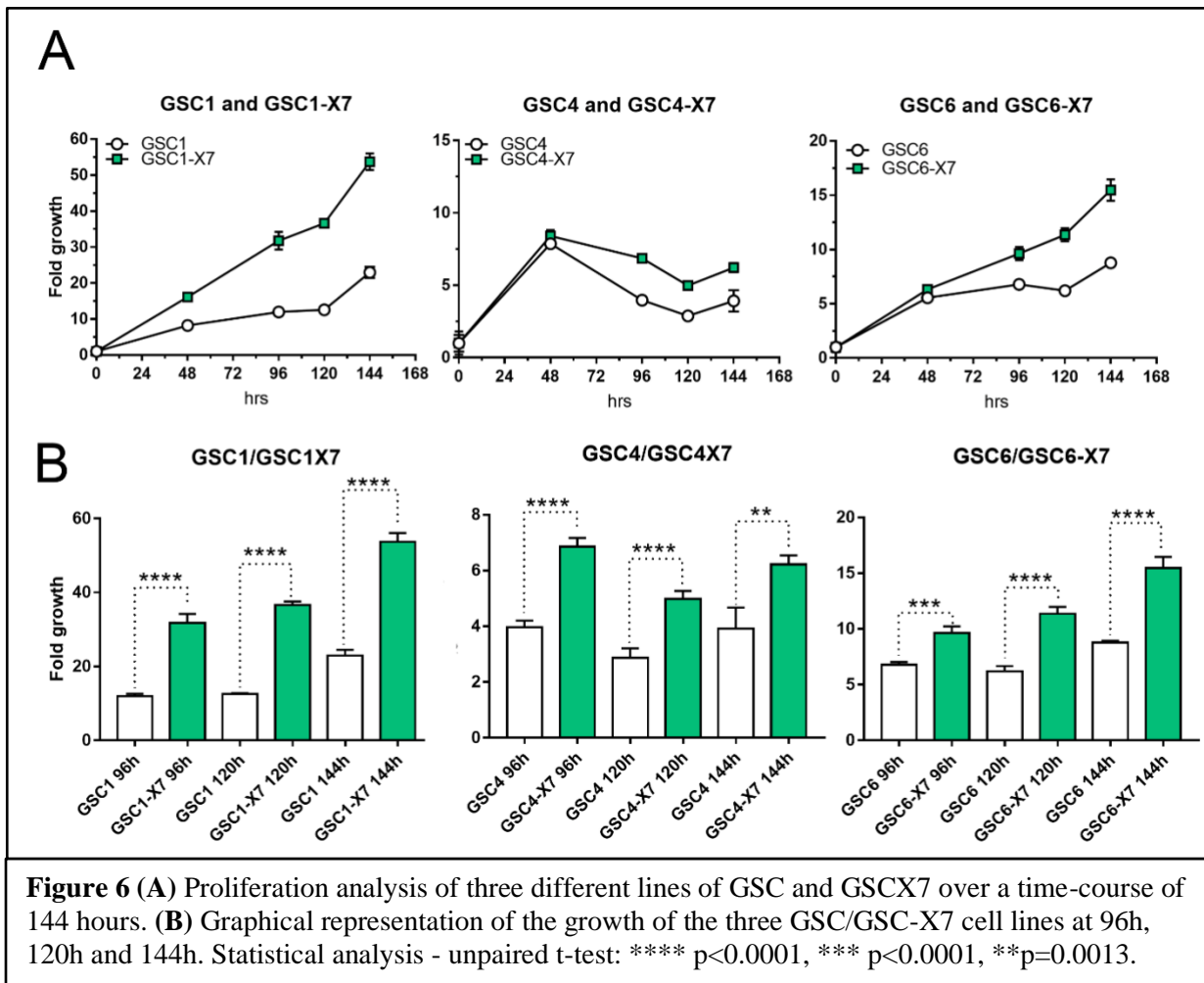
To validate expression of the CXCR7 protein on the surface of GSCs, flowcytometry analysis of GSCs was performed using a specific antibody against the human CXCR7 protein (Human CXCR7/RDC Alexa Fluor® 647-conjugated, R&D Systems FAB42273R) to stain GSCs and their CXCR7 transduced counterparts. Data was collected on the BD FACSAria™ III (Beckton Dickinson) at the University of Michigan Flowcytometry Core and analyzed using FlowJoᴛᴍ 10 Software, confirming surface expression of CXCR7 in more than 75% of the analyzed cells: GSC1-X7, GSC5-X7 (Data not shown).

We conclude therefore that CXCR7 is highly expressed in transduced cells and localized to the proper cellular compartment for functional activity.

GSCs overexpressing CXCR7 show increased proliferation *in vitro*

Studies so far have presented inconsistent results respective to the role of CXCR7 in promoting the growth of GB cells, showing either that CXCR7 does not affect the growth of GB cells (Hattermann et al., 2010) or that expression of CXCR7 promotes the growth of GB neurospheres (Walters et al., 2014).

To determine if the presence of the CXCR7 receptor alters proliferation of GSCs the growth dynamics of three different GSCs and their derived cell line overexpressing CXCR7, GSC1/GSC1-X7, GSC4/GSC4-X7 and GSC6/GSC6-X7, were analyzed over a time-course of 6 days (144h). Cells were plated onto 96 well plates at a density of 5000 cells/well in 200 microliters of NSC medium, quadruplicate wells for each cell type/time-point, and allowed to grow for 6 days. At time = 0 and every 24 hours thereafter, the relative number of GSCs/well was analyzed by measuring luminescence generated with the Cell Titer-Glo® Luminescent Cell Viability Assay. Data was analyzed and represented graphically with GraphPad Prism 7.00. Results illustrated that, while the different GSCs have a different rate of growth ranging from about 50-fold for the GSC1 to about 7 fold for GSC6, over the course of the experiment, cells overexpressing CXCR7 have increased proliferation compared to the parental cell line (**Figure 6A**). Unpaired t-test performed on the data at 96h, 120h and 144h, shows that this increased

Figure 6 (A) Proliferation analysis of three different lines of GSC and GSCX7 over a time-course of 144 hours. **(B)** Graphical representation of the growth of the three GSC/GSC-X7 cell lines at 96h, 120h and 144h. Statistical analysis - unpaired t-test: **** p<0.0001, *** p<0.0001, **p=0.0013.

growth is statistically significant after prolonged time in culture (96h, 120h, 144h, **Figure 6B and Table 2**).

	GSC1 96h	GSC1-X7 96h	GSC1 120h	GSC1-X7 120h	GSC1 144h	GSC1-X7 144h
Ave. fold increase vs T0	11.97	31.75	12.56	36.61	22.96	53.75
Fold growth GSCX7/GSC	2.65		2.91		2.34	
p value	<0.0001		<0.0001		<0.0001	
	GSC4 96h	GSC4-X7 96h	GSC4 120h	GSC4-X7 120h	GSC4 144h	GSC4-X7 144h
Ave. fold increase vs T0	3.97	6.86	2.88	4.98	3.92	6.22
Fold growth GSCX7/GSC	1.73		1.73		1.59	
p value	<0.0001		<0.0001		0.0013	
	GSC6 96h	GSC6-X7 96h	GSC6 120h	GSC6-X7 120h	GSC6 144h	GSC6-X7 144h
Ave. fold increase vs T0	6.78	9.62	6.20	11.37	8.77	15.47
Fold growth GSCX7/GSC	1.42		1.83		1.76	
p value	0.0001		<0.0001		<0.0001	

Table 2 Numerical and statistical representation of the *in vitro* growth dynamics of GSC and GSCX7 in NSC medium over a 6-day time-course.

Analysis of endogenous expression of *Cxcr4* and *Cxcr7* in GSCs and CXCR7 transduced GSCs.

To verify if there were any differences in the expression of the endogenous *Cxcl12* receptors: *Cxcr4* and *Cxcr7* between GSCs and their CXCR7 transduced counterparts, RNA was isolated from several GSC and GSC-X7 cell lines and QPCR analysis was performed using specific primers for the mouse *Cxcr4* and *Cxcr7* sequences using expression of *Hprt* as control.

These results indicated that expression of *Cxcr4* is higher when compared to expression of *Cxcr7* in GSCs from both groups of transformed NSCs: NRAS-LgT and NRAS-shp53. These results are consistent with published data showing increased CXCR4 expression in GSCs (Hattermann et al., 2010; Ping et al., 2011; Würth et al., 2014; FLüH et al., 2016). This analysis also showed that there was no significant difference in the endogenous expression of *Cxcr4* and *Cxcr7* between GSC-X7 and GSCs, in both genetic groups of GSCs (Figure 7 **(C)** and **(D)**). Considering that only two sets of NRAS-shp53 cell lines were analyzed and that individual data indicates a higher expression of both *Cxcr4* and *Cxcr7* in the CXCR7 overexpressing cells, increasing the number of cell lines analyzed in this group may ultimately reveal a statistically significant difference.
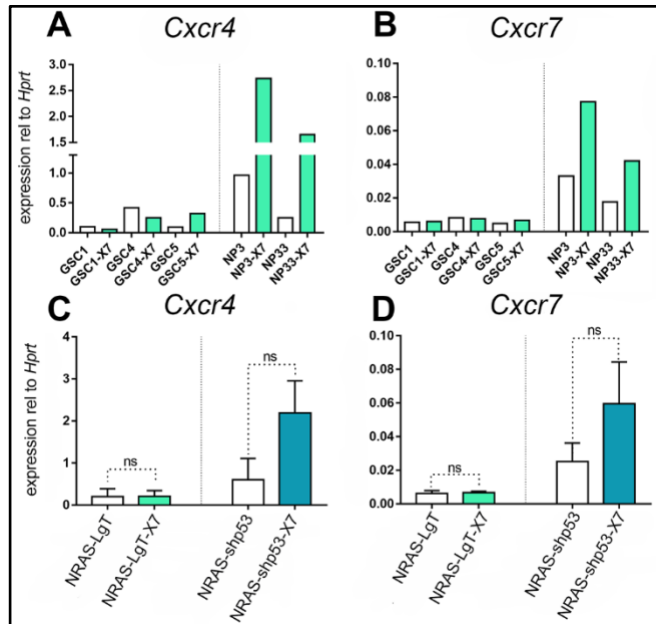
Figure 7 Expression of endogenous *Cxcr4* and *Cxcr7* in GSCs and GSC-X7. **(A)** and **(B)** are graphical representations of *Cxcr4* and *Cxcr7* expression in the individual 10 GSC cell lines analyzed. Graphs in **(C)** and **(D)** show *Cxcr4* and *Cxcr7* in the four different groups of GSCs, induced either with NRAS and LgT or with NRAS and shp53, with or without CXCR7. Statistical analysis (student t-test) shows no significant difference between groups (QPCR data).

CXCR7 induced resistance of GSCs to treatments with CXCR4 and CXCR7 inhibitors

It was previously demonstrated that the growth of GSCs after prolonged culture, under hypoxic conditions, is dependent on CXCL12 expression of which is regulated through an autocrine positive feedback mechanism (Calinescu et al., 2016). It was shown that inhibiting CXCR4 with the specific inhibitor AMD3100 abrogated the growth of GSCs and reduced expression of CXCL12.

To test if signaling through CXCR4 and/or CXCR7 modulated the growth of GSC-X7 cells, the growth of GSC5 and GSC5-X7 was analyzed after 5 days in culture (120h) in the presence or absence specific inhibitors targeting CXCR4 and CXCR7: AMD3100 and CCX771, alone or in combination. Results indicated that AMD3100 at the concentration of 20μM inhibited the viability of GSC5 by about 50%, whereas it did not affect the viability of GSC5-X7. Similarly, the CXCR7 inhibitor affected the viability of GSC5 significantly more than the one of GSC5-X7 (**Figure 8, Table 3**). The combination of CXCR4 and CXCR7 inhibitor had the biggest effect in reducing the viability of both GSC5 and GSC5-X7, but again with lower efficiency on the CXCR7 overexpressing cells. These results were surprising considering the low

26

endogenous expression of *Cxcr7* in GSC5 cells. The CXCR7 inhibitor was expected to affect the GSC-X7 cells more strongly. These results suggest that GSC-X7 may have acquired additional phenotypic changes that rendered them less sensitive to CXCR7 blockade, or that the CCX771 inhibitor exerted additional off-target effects that led to decreased viability of GSCs.
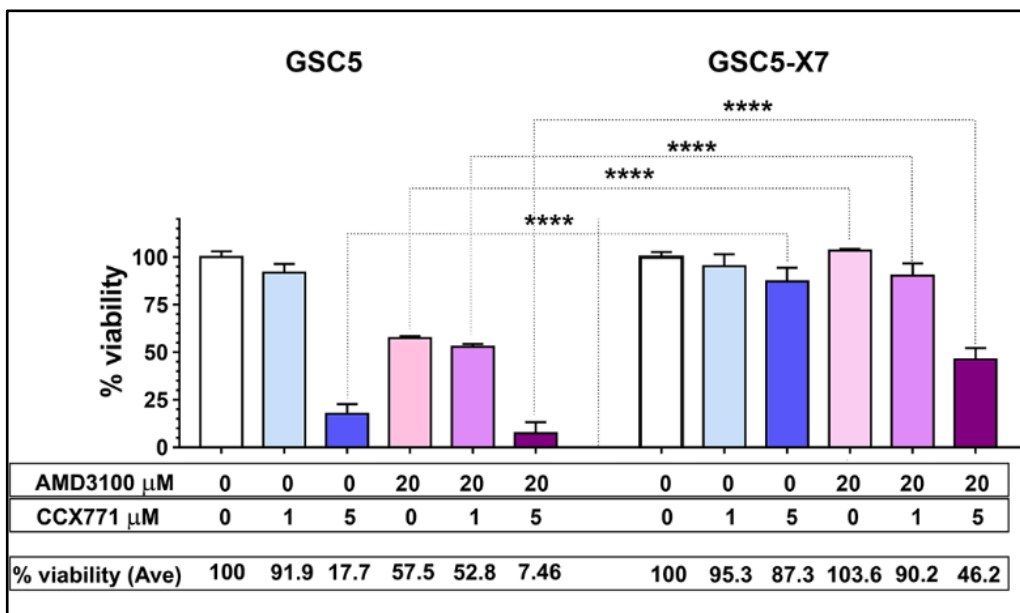
Figure 8 Viability analysis of GSC and GSC-X7 treated with CXCL12 receptor inhibitors. GSC5 and GSC5-X7 were plated at a density of 3000 cells/well onto 96 well plates in quadruplicate wells per condition and treated for 120h with the CXCR4 inhibitor AMD3100 (20μM) and the CXCR7 inhibitor CCX771 (1μM and 5μM) alone or in combination. Luminescence reads of quadruplicate wells per condition were averaged, normalized to the control wells and represented graphically as percent viability. **** $p < 0.0001$

Two-way ANOVA Tukey's multiple comparisons test (GSC5 vs. GSC5-X7)	Mean Diff.	95.00% CI of diff.	Significant?	Summary	Adjusted P Value
CCX771 1uM	-3.375	-15.36 to 8.605	No	ns	0.9969
CCX771 5uM	-69.7	-81.68 to -57.71	Yes	****	<0.0001
AMD3100 20uM	-46.05	-58.03 to -34.07	Yes	****	<0.0001
CCX771 1uM +AMD3100 20uM	-37.37	-49.35 to -25.39	Yes	****	<0.0001
CCX771 5uM+AMD3100 20uM	-38.78	-50.76 to -26.8	Yes	****	<0.0001

Table 3 Results of the statistical analysis of the viability assay presented in Figure 8 were performed with two-way ANOVA and Tukey's post-hoc multivariate test using GraphPad Prism 7.0.

To determine the half-maximal inhibitory concentration of CCX771 (IC$_{50}$) in GSCs and GSC-X7, GSC4 and GSC4-X7 were treated with increasing concentrations of CCX771, over a range spanning from 0.1 to 5 μM. After two days, cell viability was measured. Luminescence reads for GSC4 and GSC4-X7 were normalized to the control values (DMSO treated) and represented graphically with the nonlinear regression function; IC$_{50}$ and the goodness of fit (R$_2$)

were also calculated from the non-linear fit analysis using GraphPad Prism. Results presented in **Figure 9** illustrate that the IC_{50} for GSC4-X7 is higher (4.52 μM) than the one for GSC4 (1.48 μM), indicating that the CXCR7 overexpressing GSCs are more resistant to CCX771 than their parental counterpart.
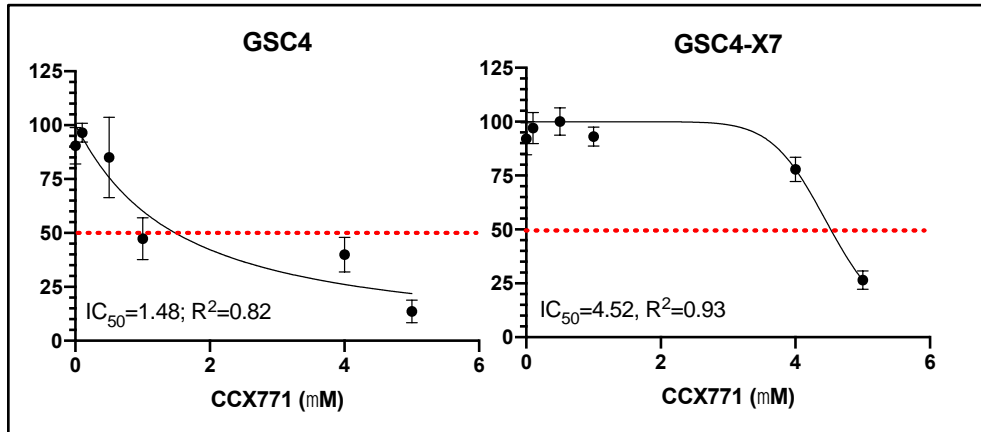
Figure 9 Analysis of the half-maximal inhibitory concentration of the CXCR7 inhibitor CCX771 (IC_{50}) in GSCs and GSC-X7. GSC4 and GSC4-X7 were plated at a density of 3000 cells/well onto 96 well plates and treated with increasing concentrations of CCX771 (0.1 to 5 mM). After two days, cell viability was measured using the Cell Titer-Glo® Luminescent Cell Viability Assay. Luminescence reads were normalized to the control values (DMSO treated) and IC_{50} and the goodness of fit (R_2) were calculated from the non-linear regression curve fit analysis using GraphPad Prism.

CXCR7 increased expression of *Cxcl12* in GSCs after prolonged culture

Since we knew that the continuous growth of GSCs after extended time in culture is dependent on the actions of the CXCL12 and intrigued by the viability data observed in the presence of CXCR4 and CXCR7 inhibition, we tested the expression of *Cxcl12* in two different GSC-X7 cell lines compared to their parental lines. GSC4, GSC4-X7, GSC5 and GSC5-X7 cells were plated onto 12 well plates at a density of $0.5 \times 10_6$ cells/ml in 2ml of NSC medium, triplicate wells per cell line. After 96h, RNA was extracted, converted into cDNA and expression of *Cxcl12* was analyzed by QPCR, using as control expression of *Hprt*. Results presented in **Figure 10** demonstrate increased expression of *Cxcl12* in GSC4-X7 and GSC5-X7 after 96h in culture, when compared to the parental cell line. Considering that CXCR7 is characterized as a scavenging receptor for CXCL12, higher expression of *Cxcl12* is surprising and may indicate that expression of *Cxcl12* in GSCs is regulated through a feedback mechanism initiated by the availability of CXCL12 in the surrounding environment.
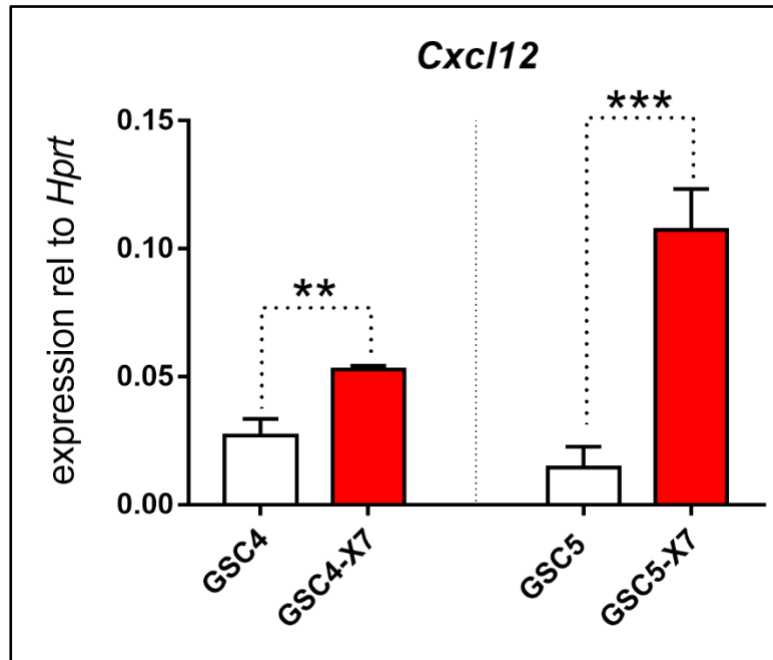
Figure 10 Expression of *Cxcl12* than the GSC and GSC-X7. Expression of *Cxcl12* was analyzed by QPCR in GSC4, GSC4-X7 and GSC5 and GSC5-X7, triplicate wells for each cell line, after 96h in culture and represented graphically as relative expression compared to *Hprt*. Statistical analysis (Student t test) was done using GraphPad Prism 7.0 software. ** p= 0.0029, *** p= 0.0009

Tested the effect of CXCR7 on the growth dynamics of GSCs *in vivo*

To determine if the presence of CXCR7 induced a proliferative advantage of GSCs in the brain of experimental mice, GSC4 and GSC4-X7 (50,000 cells, in a total volume of 2 microliters) were injected into the striatum of mice, 3 mice per cell line. To determine the sizes of the tumors that were formed, animals were euthanized two weeks after intracranial implantations, brains were perfused with a fixative, cryopreserved and sectioned in a coronal plane. Serial sections were collected to cover the entire tumor volume. Brain sections were stained with the nuclear stain 4′,6-diamidino-2-phenylindole (DAPI, 1 microgram/ml) to visualize the tumors. The tumors are easily visible with the DAPI stain, as the density of nuclei in the tumor is very high, in stark contrast to the rest of the brain. The slides with the maximum diameter of the tumor were selected for quantification for each brain. Tumor area was measured (mm2) and average tumor areas from the two groups were represented graphically **(Figure 11)**. Statistical analysis with an unpaired t-test indicates that there was no significant difference

29

between the size of the tumors induced by GSC4 and GSC4-X7 14 days after implantation (p = 0.5312).
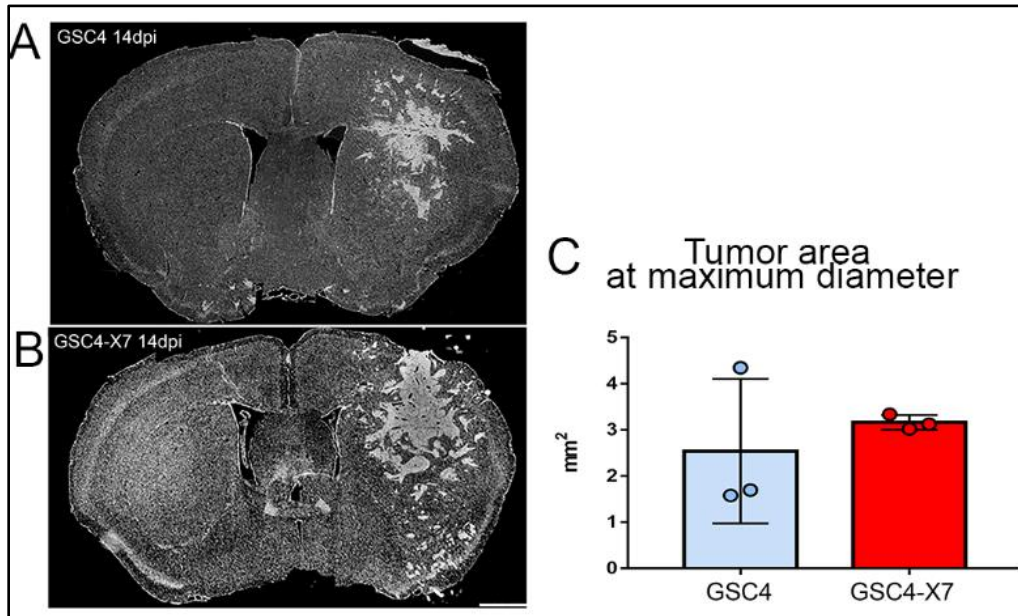
Figure 11 (A) and **(B)** Representative micrographs of coronal sections through the brain of tumor-bearing animals injected with GSC4 **(A)** or GSC4-X7 **(B).**
(C) Quantitative representation of the tumor area at the site of maximum diameter of the tumor from the two groups of mice injected either with GSC4 (blue) or with the GSC4-X7 (red). Statistical analysis: unpaired t-test, was done with GraphPad Prism 7.0 (p= 0.5312).

Discussion

Previous studies establish an important role of CXCL12 in glioblastoma progression promoting tumor growth, vascularization and radio-resistance (Rubin et al., 2003; Stevenson et al., 2008; Komatani et al., 2009; Kioi et al., 2010; Goffart et al., 2016). It was also demonstrated that CXCL12 promoted proliferation and survival of glioma stem cells under hypoxic conditions, increasing expression of factors required for cell cycle progression and inhibiting apoptosis (Calinescu et al., 2016). These effects of CXCL12 were mediated by binding to its signaling receptor CXCR4. CXCL12 can also bind to CXCR7, an atypical GPCR receptor, described to remove CXCL12 from the extracellular space and target it for degradation. It would be expected that high levels of CXCR7 will sequester CXCL12 from the extracellular space, decrease signaling through CXCR4 and inhibit progression of GB. Surprisingly, some reports present data that CXCR7 may promote progression of glioblastoma. Walters et al. demonstrated that inhibition of CXCR7 in rodent models of GB, decreased tumor size, prevented recurrence and prolonged survival of animals that were treated with irradiation following tumor implantations. Furthermore, using specimens from GB patients, the same study illustrated that high levels of CXCR7 expression correlated with increased tumor grade, suggesting that CXCR7 may promote GB progression (Walters et al., 2014).

Published studies have demonstrated that CXCR7 is primarily expressed in more differentiated GB cells and is decreased in GSCs and in the tumors of patients with recurrent disease (Hattermann et al., 2010; FLüH et al., 2016). In contrast, it was reported that expression of CXCR7 promotes the GSC phenotype and that CXCR7 blockade inhibits neurosphere formation, and this may underlie the beneficial effects of the CXCR7 inhibitor in tumor bearing animals treated with irradiation (Walters et al., 2014). To systematically address the role of CXCR7 in GSCs we generated GSCs overexpressing CXCR7 and analyzed their growth, response to CXCR4 and CXCR7 inhibitors and their production of CXCL12.

Proliferative analysis of several GSCs and GSCs overexpressing CXCR7 (GSC-X7) (**Figure 6**) indicated that CXCR7 significantly increased proliferation of GSCs. This difference was most significant after prolonged time in culture, when cells become hypoxic. It would be expected that the overexpression of CXCR7 in GSCs would result in reduced extracellular CXCL12 levels and, therefore, decreased GSC proliferation. However, surprisingly, the opposite was observed.

It was previously demonstrated that blocking CXCR4 with the small molecule inhibitor AMD3100 inhibited proliferation of GSCs after prolonged time in culture, decreasing production of CXCL12 as well as expression of genes promoting cell cycle progression. To see if the observed increase in proliferation of GSC-X7 is dependent on signaling through CXCR4 or CXCR7 we analyzed viability of GSCs and GSC-X7 in the presence of small molecule inhibitors targeting these receptors: AMD3100 and CCX771 (inhibitor of CXCR7). Surprisingly, CXCR7 expressing cells were more resistant to the actions of both inhibitors when compared to their parental counterparts (**Figures 8** and **9**). Knowing that exogenous administration of CXCL12 can rescue in part the inhibitory activity of AMD3100 on GSC survival (Calinescu et al., 2016) we next analyzed the expression of CXCL12 in GSC and GSC-X7. Results demonstrated increased expression of CXCL12 in CXCR7 overexpressing cells after prolonged culture (96h, **Figure 10**). These data indicate that expression of CXCR7 contributes to the regulation of CXCL12 expression, through a sensitive feedback mechanism that may depend on CXCL12 internalization and degradation. CXCR7 may bind to CXCL12, induce receptor-ligand sequestration and decrease the extracellular CXCL12 concentration; however, the feedback mechanism will result in increased production of CXCL12 to replenish those lost. Therefore, the increased resistance of GSCX7 to CCX771 (**Figure 9**) could be explained by the increased production of CXCL12 and a possibly higher turnover of CXCR7 receptor. Cells that are constantly producing CXCL12 and have rapid turnover of CXCR7 can bind to either CCX771 or CXCL12. Binding to CXCL12 would activate downstream pathways to promote cell growth (**Figure 6**).

Further experiments could test if the presence of CXCL12 is indeed driving increased proliferation of GSC-X7. Function blocking antibodies against CXCL12 over a range of concentrations could be used on their own or in combination with CCX771. If resistance to CCX771 is due to the increased production of CXCL12, partial blocking of CXCL12 may increase sensitivity to CCX771 and decrease viability of GSC-X7 more strongly in the presence of the function blocking antibodies; this will indicate that resistance to CCX771 in GSC-X7 was indeed dependent on the levels of CXCL12. An alternate approach could be to generate GSCs that do not express CXCL12 using CRISPR/Cas9 mediated deletion for example. The experiment would be performed using the same procedure described above with or without addition of exogenous CXCL12.

To test if resistance to CCX771 is dependent on a higher turnover of the CXCR7 receptors, one can block the recycling endosomes with primaquine (Luker et al., 2010) and see if that would increase sensitivity to CCX771 in CXCR7 overexpressing cells. If inhibiting CXCL12 function or CXCR7 turnover would not result in a change of sensitivity to CCX771, then the results could be explained by off-target effects of the CCX771 inhibitor. In this manner, function blocking antibodies against CXCR7 could be used to test the role of CXCR7 on the survival and proliferation of GSCs.

To gain further insight into the mechanism of increased survival and/or proliferation of GSC-X7, additional experiments could test if the presence of CXCR7 increases expression of cell cycle promoting genes: *CCND1* (*Cyclin D1*), *Cdk4*, *CDk6,* inhibits apoptosis, activates the PI3K pathway and is indeed correlated with hypoxia, assessed by expression of HIF1α. Results of these experiments will establish if signaling through CXCR7 in GSCs has similar consequences as the ones described for signaling through CXCR4 (Calinescu et al., 2016). As shown in Fig.7 endogenous expression of *Cxcr4* in GSCs is 10-20 fold higher than endogenous expression of *Cxcr7*. It could be possible that overexpression of CXCR7 results in formation of CXCR4/CXCR7 heterodimers and that the effects observed are due to signaling through these heterodimer receptors. To determine if the observed results stem from signaling through CXCR4/CXCR7 heterodimers, we could generate CXCR4 deficient GSCs and analyze proliferation, response to inhibitors and downstream cellular effects GSC-X7.

Finally, results from the *in vivo* experiments with GSC and GSC-X7 implanted into the brain of mice indicated that there is no significant difference between the growth dynamics of these GSCs after 14 days. (**Figure 11**). These results are inconsistent with the results from the *in vitro* experiments. Limitation of the *in vivo* experiment is that so far, we only analyzed three animals at 14 days post implantation and only with one cell line.

It is possible that, after prolonged growth *in vivo*, similar to the *in vitro* experiments, the tumors would become hypoxic and the presence of the CXCR7 receptor will result in increased CXCL12 production that would stimulate tumor growth. Experiments analyzing tumor growth at later timepoints would illustrate if this would indeed be the case.

Increasing the sample size of the experimental groups will also increase confidence in the experimental results. Future experiments could analyze the overall survival of multiple mice injected with several GSCs or GSC-X7 cell lines and assess the reproducibility of the

experimental outcomes. It would be expected that mice injected with GSC-X7s will have decreased survival time because of the autocrine feedback mechanism. However, the complex *in vivo* environment in the brain, the presence of neighboring neurons, glia, vascular cells and infiltrating immune cells are likely to alter the tumor microenvironment and modulate the growth of GSCs and GSC-X7 cells. For example, CXCR7 is highly expressed in the tumor vasculature, and may compete with binding of CXCL12 to GSCs. In this case, CXCL12 will function in a paracrine way and may alter the level of vascularization in the tumors. A comprehensive *in vivo* analysis of tumor progression using GSC and GSC-X7 will be paramount to determine the role of CXCR7 on GSCs in GB progression. Provided that the long-term effects of the CXCR7 inhibitor are specific, treatment of tumor-bearing animals (GSC or GSC-X7) with the CXCR7 inhibitor will further establish if this therapeutic approach would be beneficial for GB patients. Considering the *in vitro* data demonstrating that combined treatment with AMD3100 and CCX771 induced the maximum decrease in tumor cell viability, this approach could be tested *in vivo* to determine if it would result in increased survival of tumor-bearing animals.

In summary, our data so far show that GSCs overexpressing CXCR7 have an increased proliferative capacity after long term culture, produce more CXCL12 and have increased resistance to CXCR4 and CXCR7 inhibitors. In contrast to *in vitro* experiments, so far, experiments *in vivo* have not demonstrated enhanced growth of GSC-X7 tumors in mice. Our data confirm that CXCL12 plays an important role in the survival and proliferation of GSCs, especially in hypoxic conditions, after long term culture. Results suggest the existence of a complex autocrine feedback mechanism that modulates expression of CXCL12 and is regulated, at least in part, by levels of CXCR7. In addition, the combinatorial treatment with both CXCR4 and CXCR7 inhibitors was most effective in reducing GSC viability *in vitro*. Future experiments will further dissect the cellular and molecular mechanisms that result in increased CXCL12 production and resistance to small molecule inhibitors observed in GSC-X7. A detailed understanding of the mechanisms that govern CXCL12 biology in GSCs will allow the design of specific therapeutic agents to target GSCs, important contributors to treatment failure and recurrence of glioblastoma.

References

Agnihotri S, Burrell KE, Wolf A, Jalali S, Hawkins C, Rutka JT, Zadeh G (2013) Glioblastoma, a brief review of history, molecular genetics, animal models and novel therapeutic strategies. Archivum immunologiae et therapiae experimentalis 61:25-41.

Auffinger B, Tobias A, Han Y, Lee G, Guo D, Dey M, Lesniak M, Ahmed A (2014) Conversion of differentiated cancer cells into cancer stem-like cells in a glioblastoma model after primary chemotherapy. Cell death and differentiation 21:1119.

Balabanian K, Lagane B, Infantino S, Chow KY, Harriague J, Moepps B, Arenzana-Seisdedos F, Thelen M, Bachelerie F (2005) The chemokine SDF-1/CXCL12 binds to and signals through the orphan receptor RDC1 in T lymphocytes. Journal of Biological Chemistry 280:35760-35766.

Bao S, Wu Q, Li Z, Sathornsumetee S, Wang H, McLendon RE, Hjelmeland AB, Rich JN (2008) Targeting cancer stem cells through L1CAM suppresses glioma growth. Cancer research 68:6043-6048.

Bao S, Wu Q, McLendon RE, Hao Y, Shi Q, Hjelmeland AB, Dewhirst MW, Bigner DD, Rich JN (2006a) Glioma stem cells promote radioresistance by preferential activation of the DNA damage response. nature 444:756.

Bao S, Wu Q, Sathornsumetee S, Hao Y, Li Z, Hjelmeland AB, Shi Q, McLendon RE, Bigner DD, Rich JN (2006b) Stem cell–like glioma cells promote tumor angiogenesis through vascular endothelial growth factor. Cancer research 66:7843-7848.

Beier D, Schulz JB, Beier CP (2011) Chemoresistance of glioblastoma cancer stem cells-much more complex than expected. Molecular cancer 10:128.

Burns JM, Summers BC, Wang Y, Melikian A, Berahovich R, Miao Z, Penfold ME, Sunshine MJ, Littman DR, Kuo CJ, Wei K, McMaster BE, Wright K, Howard MC, Schall TJ (2006) A novel chemokine receptor for SDF-1 and I-TAC involved in cell survival, cell adhesion, and tumor development. J Exp Med 203:2201-2213.

Calinescu A-A, Núñez FJ, Koschmann C, Kolb BL, Lowenstein PR, Castro MG (2015) Transposon mediated integration of plasmid DNA into the subventricular zone of neonatal mice to generate novel models of glioblastoma. JoVE (Journal of Visualized Experiments):e52443.

Calinescu AA, Yadav VN, Carballo E, Kadiyala P, Tran D, Zamler D, Doherty R, Srikanth M, Lowenstein PR, Castro MG (2016) Survival and proliferation of neural progenitor derived glioblastomas under hypoxic stress is controlled by a CXCL12/CXCR4 autocrine positive feedback mechanism. Clinical cancer research : an official journal of the American Association for Cancer Research.

Domanska UM, Kruizinga RC, Nagengast WB, Timmer-Bosscha H, Huls G, de Vries EG, Walenkamp AM (2013) A review on CXCR4/CXCL12 axis in oncology: no place to hide. European journal of cancer 49:219-230.

Duda DG, Kozin SV, Kirkpatrick ND, Xu L, Fukumura D, Jain RK (2011) CXCL12 (SDF1α)-CXCR4/CXCR7 pathway inhibition: an emerging sensitizer for anticancer therapies? Clinical cancer research 17:2074-2080.

Esencay M, Sarfraz Y, Zagzag D (2013) CXCR7 is induced by hypoxia and mediates glioma cell migration towards SDF-1α. BMC cancer 13:347.

Ferguson SS (2001) Evolving concepts in G protein-coupled receptor endocytosis: the role in receptor desensitization and signaling. Pharmacological reviews 53:1-24.

FLüH C, Hattermann K, Mehdorn HM, Synowitz M, Held-Feindt J (2016) Differential expression of CXCR4 and CXCR7 with various stem cell markers in paired human primary and recurrent glioblastomas. International journal of oncology 48:1408-1416.

Freitas C, Desnoyer A, Meuris F, Bachelerie F, Balabanian K, Machelon V (2014) The relevance of the chemokine receptor ACKR3/CXCR7 on CXCL12-mediated effects in cancers with a focus on virus-related cancers. Cytokine & growth factor reviews 25:307-316.

Gan HK, Kaye AH, Luwor RB (2009) The EGFRvIII variant in glioblastoma multiforme. Journal of Clinical Neuroscience 16:748-754.

Goffart N, Kroonen J, Di Valentin E, Dedobbeleer M, Denne A, Martinive P, Rogister B (2014) Adult mouse subventricular zones stimulate glioblastoma stem cells specific invasion through CXCL12/CXCR4 signaling. Neuro-oncology 17:81-94.

Goffart N, Lombard A, Lallemand F, Kroonen J, Nassen J, Di Valentin E, Berendsen S, Dedobbeleer M, Willems E, Robe P (2016) CXCL12 mediates glioblastoma resistance to radiotherapy in the subventricular zone. Neuro-oncology 19:66-77.

Guo J-C, Li J, Zhou L, Yang J-Y, Zhang Z-G, Liang Z-Y, Zhou W-X, You L, Zhang T-P, Zhao Y-P (2016) CXCL12-CXCR7 axis contributes to the invasive phenotype of pancreatic cancer. Oncotarget 7:62006.

Hattermann K, Mentlein R (2013) An infernal trio: the chemokine CXCL12 and its receptors CXCR4 and CXCR7 in tumor biology. Annals of Anatomy-Anatomischer Anzeiger 195:103-110.

Hattermann K, Held-Feindt J, Lucius R, Müerköster SS, Penfold ME, Schall TJ, Mentlein R (2010) The chemokine receptor CXCR7 is highly expressed in human glioma cells and mediates antiapoptotic effects. Cancer research 70:3299-3308.

Heimberger AB, Suki D, Yang D, Shi W, Aldape K (2005) The natural history of EGFR and EGFRvIII in glioblastoma patients. Journal of translational medicine 3:38.

Holland EC (2001) Gliomagenesis: genetic alterations and mouse models. Nature Reviews Genetics 2:120-129.

Hottinger AF, Stupp R, Homicsko K (2014) Standards of care and novel approaches in the management of glioblastoma multiforme. Chinese journal of cancer 33:32.

Huang J, Yu J, Tu L, Huang N, Li H, Luo Y (2019) Isocitrate dehydrogenase mutations in glioma: From basic discovery to therapeutics development. Frontiers in oncology 9:506.

Killela PJ, Pirozzi CJ, Healy P, Reitman ZJ, Lipp E, Rasheed BA, Yang R, Diplas BH, Wang Z, Greer PK (2014) Mutations in IDH1, IDH2, and in the TERT promoter define clinically distinct subgroups of adult malignant gliomas. Oncotarget 5:1515.

Kioi M, Vogel H, Schultz G, Hoffman RM, Harsh GR, Brown JM (2010) Inhibition of vasculogenesis, but not angiogenesis, prevents the recurrence of glioblastoma after irradiation in mice. The Journal of clinical investigation 120:694-705.

Komatani H, Sugita Y, Arakawa F, Ohshima K, Shigemori M (2009) Expression of CXCL12 on pseudopalisading cells and proliferating microvessels in glioblastomas: an accelerated growth factor in glioblastomas. International journal of oncology 34:665-672.

Lee EQ, Duda DG, Muzikansky A, Gerstner ER, Kuhn JG, Reardon DA, Nayak L, Norden AD, Doherty L, LaFrankie D (2018) Phase I and biomarker study of plerixafor and bevacizumab in recurrent high-grade glioma. Clinical Cancer Research 24:4643-4649.

Levoye A, Balabanian K, Baleux F, Bachelerie F, Lagane B (2009) CXCR7 heterodimerizes with CXCR4 and regulates CXCL12-mediated G protein signaling. Blood 113:6085-6093.

Ligon KL, Huillard E, Mehta S, Kesari S, Liu H, Alberta JA, Bachoo RM, Kane M, Louis DN, DePinho RA (2007) Olig2-regulated lineage-restricted pathway controls replication competence in neural stem cells and malignant glioma. Neuron 53:503-517.

Liu G, Yuan X, Zeng Z, Tunici P, Ng H, Abdulkadir IR, Lu L, Irvin D, Black KL, John SY (2006) Analysis of gene expression and chemoresistance of CD133+ cancer stem cells in glioblastoma. Molecular cancer 5:67.

Luker KE, Gupta M, Luker GD (2009) Bioluminescent CXCL12 fusion protein for cellular studies of CXCR4 and CXCR7. Biotechniques 47:625-632.

Luker KE, Steele JM, Mihalko LA, Ray P, Luker GD (2010) Constitutive and chemokine-dependent internalization and recycling of CXCR7 in breast cancer cells to degrade chemokine ligands. Oncogene 29:4599-4610.

Luttrell LM (2008) Reviews in molecular biology and biotechnology: transmembrane signaling by G protein-coupled receptors. Molecular biotechnology 39:239-264.

Miao Z, Luker KE, Summers BC, Berahovich R, Bhojani MS, Rehemtulla A, Kleer CG, Essner JJ, Nasevicius A, Luker GD (2007) CXCR7 (RDC1) promotes breast and lung tumor growth in vivo and is expressed on tumor-associated vasculature. Proceedings of the National Academy of Sciences 104:15735-15740.

Naumann U, Cameroni E, Pruenster M, Mahabaleshwar H, Raz E, Zerwes HG, Rot A, Thelen M (2010) CXCR7 functions as a scavenger for CXCL12 and CXCL11. PLoS One 5:e9175.

Neilsen BK, Sleightholm R, McComb R, Ramkissoon SH, Ross JS, Corona RJ, Miller VA, Cooke M, Aizenberg MR (2019) Comprehensive genetic alteration profiling in primary and recurrent glioblastoma. Journal of neuro-oncology 142:111-118.

Network CGAR (2008) Comprehensive genomic characterization defines human glioblastoma genes and core pathways. Nature 455:1061.

Ostrom QT, Cote DJ, Ascha M, Kruchko C, Barnholtz-Sloan JS (2018) Adult glioma incidence and survival by race or ethnicity in the United States from 2000 to 2014. JAMA oncology 4:1254-1262.

Ostrom QT, Gittleman H, Xu J, Kromer C, Wolinsky Y, Kruchko C, Barnholtz-Sloan JS (2016) CBTRUS statistical report: primary brain and other central nervous system tumors diagnosed in the United States in 2009–2013. Neuro-oncology 18:v1-v75.

Parsons DW, Jones S, Zhang X, Lin JC-H, Leary RJ, Angenendt P, Mankoo P, Carter H, Siu I-M, Gallia GL (2008) An integrated genomic analysis of human glioblastoma multiforme. science 321:1807-1812.

Peitzsch C, Cojoc M, Kurth I, Dubrovska A (2015) Implications of CXCR4/CXCL12 Interaction for Cancer Stem Cell Maintenance and Cancer Progression. In: Cancer Stem Cells: Emerging Concepts and Future Perspectives in Translational Oncology, pp 89-130: Springer.

Pfaffl MW (2001) A new mathematical model for relative quantification in real-time RT–PCR. Nucleic acids research 29:e45-e45.

Pierce KL, Premont RT, Lefkowitz RJ (2002) Seven-transmembrane receptors. Nature reviews Molecular cell biology 3:639-650.

Ping Yf, Yao Xh, Jiang Jy, Zhao Lt, Yu Sc, Jiang T, Lin MC, Chen Jh, Wang B, Zhang R (2011) The chemokine CXCL12 and its receptor CXCR4 promote glioma stem cell-mediated VEGF production and tumour angiogenesis via PI3K/AKT signalling. The Journal of pathology 224:344-354.

Qian T, Liu Y, Dong Y, Zhang L, Dong Y, Sun Y, Sun D (2018) CXCR7 regulates breast tumor metastasis and angiogenesis in vivo and in vitro. Molecular medicine reports 17:3633-3639.

Rajagopal S, Kim J, Ahn S, Craig S, Lam CM, Gerard NP, Gerard C, Lefkowitz RJ (2010) β-arrestin-but not G protein-mediated signaling by the "decoy" receptor CXCR7. Proceedings of the National Academy of Sciences 107:628-632.

Rojiani AM, Dorovini-Zis K (1996) Glomeruloid vascular structures in glioblastoma multiforme: an immunohistochemical and ultrastructural study. Journal of neurosurgery 85:1078-1084.

Rubin JB, Kung AL, Klein RS, Chan JA, Sun Y, Schmidt K, Kieran MW, Luster AD, Segal RA (2003) A small-molecule antagonist of CXCR4 inhibits intracranial growth of primary brain tumors. Proceedings of the National Academy of Sciences 100:13513-13518.

Sánchez-Martín L, Sánchez-Mateos P, Cabañas C (2013) CXCR7 impact on CXCL12 biology and disease. Trends in molecular medicine 19:12-22.

Sierro F, Biben C, Martínez-Muñoz L, Mellado M, Ransohoff RM, Li M, Woehl B, Leung H, Groom J, Batten M (2007) Disrupted cardiac development but normal hematopoiesis in mice deficient in the second CXCL12/SDF-1 receptor, CXCR7. Proceedings of the National Academy of Sciences 104:14759-14764.

Singh SK, Clarke ID, Terasaki M, Bonn VE, Hawkins C, Squire J, Dirks PB (2003) Identification of a cancer stem cell in human brain tumors. Cancer research 63:5821-5828.

Stacer AC, Fenner J, Cavnar SP, Xiao A, Zhao S, Chang SL, Salomonnson A, Luker KE, Luker GD (2016) Endothelial CXCR7 regulates breast cancer metastasis. Oncogene 35:1716.

Stevenson CB, Ehtesham M, McMillan KM, Valadez JG, Edgeworth ML, Price RR, Abel TW, Mapara KY, Thompson RC (2008) CXCR4 expression is elevated in glioblastoma multiforme and correlates with an increase in intensity and extent of peritumoral T2-weighted magnetic resonance imaging signal abnormalities. Neurosurgery 63:560-570.

Stiles CD, Rowitch DH (2008) Glioma stem cells: a midterm exam. Neuron 58:832-846.

Stupp R, Mason WP, Van Den Bent MJ, Weller M, Fisher B, Taphoorn MJ, Belanger K, Brandes AA, Marosi C, Bogdahn U (2005) Radiotherapy plus concomitant and adjuvant temozolomide for glioblastoma. New England Journal of Medicine 352:987-996.

Tabatabai G, Frank B, Möhle R, Weller M, Wick W (2006) Irradiation and hypoxia promote homing of haematopoietic progenitor cells towards gliomas by TGF-β-dependent HIF-1α-mediated induction of CXCL12. Brain 129:2426-2435.

Thomas RP, Nagpal S, Iv M, Soltys SG, Bertrand S, Pelpola JS, Yang J, Ball RL, Brown M, Recht LD (2018) CXCR4 blockade at the end of irradiation to improve local control of glioblastoma (GBM). In: American Society of Clinical Oncology.

Torossian F, Anginot A, Chabanon A, Clay D, Guerton B, Desterke C, Boutin L, Marullo S, Scott MG, Lataillade J-J (2014) CXCR7 participates in CXCL12-induced CD34+ cell cycling through β-arrestin–dependent Akt activation. Blood, The Journal of the American Society of Hematology 123:191-202.

Ulvmar MH, Hub E, Rot A (2011) Atypical chemokine receptors. Experimental cell research 317:556-568.

Walters M, Ebsworth K, Berahovich R, Penfold M, Liu S, Al Omran R, Kioi M, Chernikova S, Tseng D, Mulkearns-Hubert E (2014) Inhibition of CXCR7 extends survival following irradiation of brain tumours in mice and rats. British journal of cancer 110:1179.

Wang J, Shiozawa Y, Wang J, Wang Y, Jung Y, Pienta KJ, Mehra R, Loberg R, Taichman RS (2008) The role of CXCR7/RDC1 as a chemokine receptor for CXCL12/SDF-1 in prostate cancer. Journal of Biological Chemistry 283:4283-4294.

Weller M, Watts C, Reardon DA, Mehta MP (2019) Glioblastoma. In: Oncology of CNS Tumors, pp 237-247: Springer.

Wu Y, Tang S, Sun G, Sun K (2016) CXCR7 mediates TGFβ1-promoted EMT and tumor-initiating features in lung cancer. Oncogene 35:2123.

Würth R, Bajetto A, Harrison JK, Barbieri F, Florio T (2014) CXCL12 modulation of CXCR4 and CXCR7 activity in human glioblastoma stem-like cells and regulation of the tumor microenvironment. Frontiers in cellular neuroscience 8:144.

Yan H, Parsons DW, Jin G, McLendon R, Rasheed BA, Yuan W, Kos I, Batinic-Haberle I, Jones S, Riggins GJ (2009) IDH1 and IDH2 mutations in gliomas. New England journal of medicine 360:765-773.

Zagzag D, Lukyanov Y, Lan L, Ali MA, Esencay M, Mendez O, Yee H, Voura EB, Newcomb EW (2006) Hypoxia-inducible factor 1 and VEGF upregulate CXCR4 in glioblastoma: implications for angiogenesis and glioma cell invasion. Laboratory investigation 86:1221-1232.

Zheng K, Li H-Y, Su X-L, Wang X-Y, Tian T, Li F, Ren G-S (2010) Chemokine receptor CXCR7 regulates the invasion, angiogenesis and tumor growth of human hepatocellular carcinoma cells. Journal of Experimental & Clinical Cancer Research 29:31.

Appendix
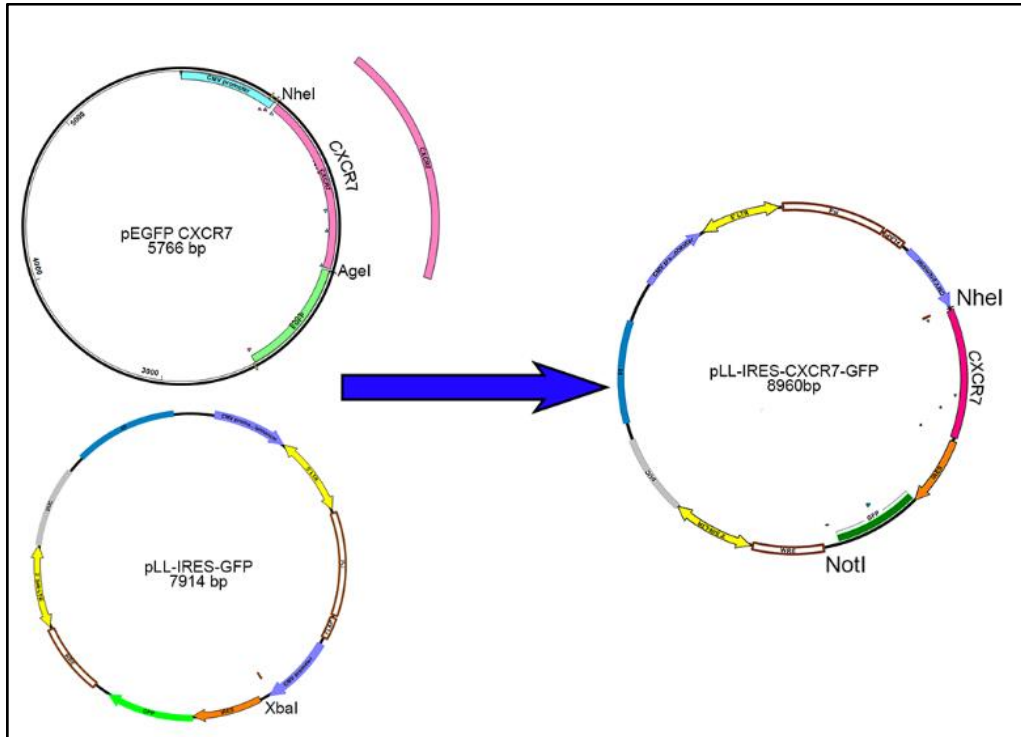
Supplementary Figure 1. Schematic representation of the subcloning strategy to release the CXCR7 open reading frame from the pEGFP-CXCR7 plasmid and insert it into the lentiviral vector pLL-IRES-GFP.
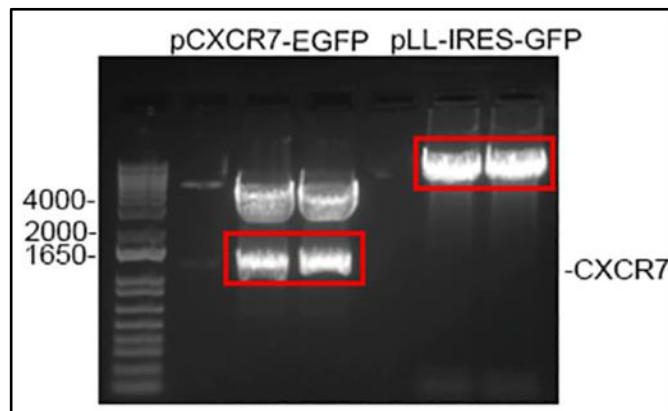
Supplementary Figure 2. Agarose electrophoresis of restriction digest reactions to release the HCXCR7 fragment and liniarize the pLL-IRES-GFP vector. Restriction digest of ten micrograms of plasmid and pLL-IRES-GFP was performed overnight with NheI and AgeI (for pCXCR7-EGFP) and XbaI (for pLL-IRES-GFP) respectively. Expected size of the CXCR7 insert was 1085 bp. Digests were resolved by gel electrophoresis and bands visualized with an UV transilluminator. Insert and vector (red rectangle areas) were cut, gel purified and used for the ligation reactions.
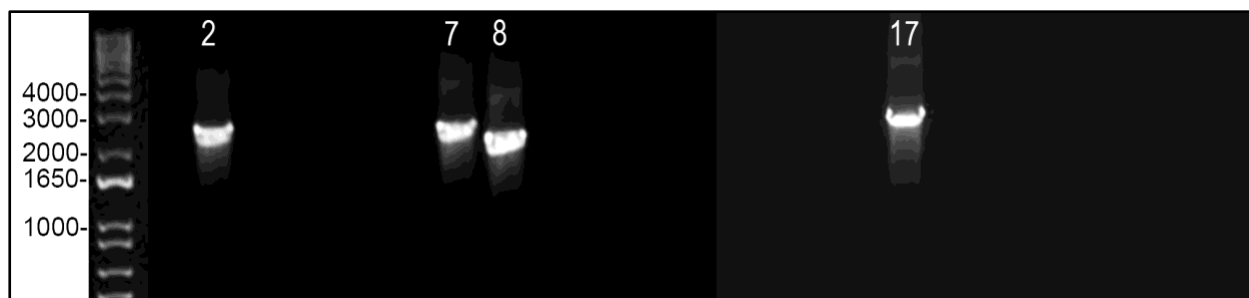
Supplementary Figure 3. Agarose electrophoresis of PCR reactions assembled with cultures from transformed bacteria. Ligation reactions with the linearized, blunted and dephosphorylated and purified vector: pLL-IRES-GFP and the blunted and purified insert: HCXCR7 were used to transform chemically competent E. coli. Twenty-four colonies were selected and cultured for 2-3 hours in 1 ml of Luria Broth. These cultures were used as template for PCR reactions with the HCXCR7 F1 and EGFP R1 primers, to check for transformants carrying the desired plasmid. PCR reactions were resolved by agarose. Results show that colonies 2, 7, 8 and 17 have amplification products in the expected range (2388bp).
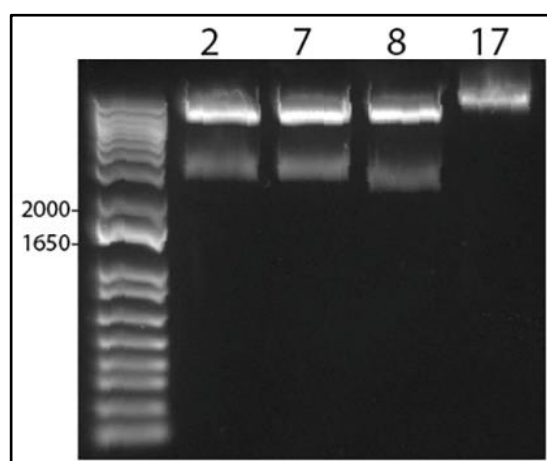
Supplementary Figure 4. Agarose gel electrophoresis of diagnostic restriction digest of DNA from colonies 2,7,8 and 17. DNA was extracted from the bacterial cultures of colonies 2, 7, 8 and 17 and a diagnostic restriction digest was performed using the NotI and NheI enzymes, to release the inserted HCXCR7 fragment. Reactions were resolved by gel electrophoresis and results illustrate that colonies 2, 7, 8 released the fragment, whereas colony 17 did not.

5'ATGGATCTGCATCTCTTCGACTACTCAGAGCCAGGGAACTTCTCGGACATCAGCTGGCCATGCAACAGCAGCGACTGCAT
CGTGGTGGACACGGTGATGTGTCCCAACATGCCCAACAAAAGCGTCCTGCTCTACACGCTCTCCTTCATTTACATTTTCATC
TTCGTCATCGGCATGATTGCCAACTCCGTGGTGGTCTGGGTGAATATCCAGGCCAAGACCACAGGCTATGACACGCACTGC
TACATCTTGAACCTGGCCATTGCCGACCTGTGGGTTGTCCTCACCATCCCAGTCTGGGTGGTCAGTCTCGTGCAGCACAACC
AGTGGCCCATGGGCGAGCTCACGTGCAAAGTCACACACCTCATCTTCTCCATCAACCTCTTCGGCAGCATTTTCTTCCTCAC
GTGCATGAGCGTGGACCGCTACCTCTCCATCACCTACTTCACCAACACCCCCAGCAGCAGGAAGAAGATGGTACGCCGTGT
CGTCTGCATCCTGGTGTGGCTGCTGGCCTTCTGCGTGTCTCTGCCTGACACCTACTACCTGAAGACCGTCACGTCTGCGTCC
AACAATGAGACCTACTGCCGGTCCTTCTACCCCGAGCACAGCATCAAGGAGTGGCTGATCGGCATGGAGCTGGTCTCCGTT
GTCTTGGGCTTTGCCGTTCCCTTCTCCATTGTCGCTGTCTTCTACTTCCTGCTGGCCAGAGCCATCTCGGCGTCCAGTGACCA
GGAGAAGCACAGCAGCCGGAAGATCATCTTCTCCTACGTGGTGGTCTTCCTTGTCTGCTGGTTGCCCTACCACGTGGCGGT
GCTGCTGGACATCTTCTCCATCCTGCACTACATCCCTTTCACCTGCCGGCTGGAGCACGCCCTCTTCACGGCCCTGCATGTC
ACACAGTGCCTGTCGCTGGTGCACTGCTGCGTCAACCCTGTCCTCTACAGCTTCATCAATCGCAACTACAGGTACGAGCTG
ATGAAGGCCTTCATCTTCAAGTACTCGGCCAAAACAGGGCTCACCAAGCTCATCGATGCCTCCAGAGTCTCAGAGACGGAG
TACTCTGCCTTGGAGCAGAGCACCAAACTAGAGTGCAGTTCTTAGAAGGCTTGCAGGAGATCCGCCCCTCTCCCTCCCCCC
CCCCTAACGTTACTGGCCGAAGCCGCTTGGAATAAGGCCGGTGTGCGTTTGTCTATATGTTATTTTCCACCATATTGCCGTC
TTTTGGCAATGTGAGGGCCCGGAAACCTGGCCCTGTCTTCTTGACGAGCATTCCTAGGGGTCTTTCCCCTCTCGCCAAAGGA
ATGCAAGGTCTGTTGAATGTCGTGAAGGAAGCAGTTCCTCTGGAAGCTTCTTGAAGACAAACAACGTCTGTAGCGACCCTT
TGCAGGCAGCGGAACCCCCCACCTGGCGACAGGTGCCTCTGCGGCCAAAAGCCACGTGTATAAGATACACCTGCAAAGGC
GGCACAACCCCAGTGCCACGTTGTGAGTTGGATAGTTGTGGAAAGAGTCAAATGGCTCTCCTCAAGCGTATTCAACAAGGG
GCTGAAGGATGCCCAGAAGGTACCCCATTGTATGGGATCTGATCTGGGGCCTCGGTGCACATGCTTTACATGTGTTTAGTC
GAGGTTAAAAAAACGTCTAGGCCCCCCGAACCACGGGGACGTGGTTTTCCTTTGAAAAACACGATGATAATATGGCCACA
ACCATGGTGAGCAAGGGCGAGGAGCTGTTCACCGGGGTGGTGCCCATCCTGGTCGAGCTGGACGGCGACGTAAACGGCCA
CAAGTTCAGCGTGTCCGGCGAGGGCGAGGGCGATGCCACCTACGGCAAGCTGACCCTGAAGTTCATCTGCACCACCGGCA
AGCTGCCCGTGCCCTGGCCCACCCTCGTGACCACCCTGACCTACGGCGTGCAGTGCTTCAGCCGCTACCCCGACCACATGA
AGCAGCACGACTTCTTCAAGTCCGCCATGCCCGAAGGCTACGTCCAGGAGCGCACCATCTTCTTCAAGGACGACGGCAACT
ACAAGACCCGCGCCGAGGTGAAGTTCGAGGGCGACACCCTGGTGAACCGCATCGAGCTGAAGGGCATCGACTTCAAGGAG
GACGGCAACATCCTGGGGCACAAGCTGGAGTACAACTACAACAGCCACAACGTCTATATCATGGCCGACAAGCAGAAGAA
CGGCATCAAGGTGAACTTCAAGATCCGCCACAACATCGAGGACGGCAGCGTGCAGCTCGCCGACCACTACCAGCAGAACA
CCCCCATCGGCGACGGCCCCGTGCTGCTGCCCGACAACCACTACCTGAGCACCCAGTCCGCCCTGAGCAAAGACCCCAACG
AGAAGCGCGATCACATGGTCCTGCTGGAGTTCGTGACCGCCGCCGGGATCACTCTCGGCATGGACGAGCTGTACAAGTAA
AGCGG 3'

Supplementary Figure 5. Sequencing result of the resulting pLL-IRES-CXCR7-GFP plasmid including the nucleotides from CXCR7 to the end of the EGFP sequence of the ligated vector. The blue sequence is CXCR7 and the green sequence is GFP. The red sequences at the 5' and 3' ends are the DNA binding sites for the forward primer and reverse primers.

List of Materials Used

Supplementary Table 1. List of materials used

Category	Reagent	Company	Catalog number	Experiment used
Plasmid	pLentilox-IRES-GFP	UM Vector Core	N/A	Subcloning of CXCR7
Plasmid	pEGFP-CXCR7	Gift from Drs. Kathy and Gary Luker	N/A	Subcloning of CXCR7
Plasmid	pLentilox-CXCR7-IRES-GFP	Generated in the lab	N/A	Transduction of GSCs
Reagent	NEB® Turbo Competent E. coli (High Efficiency)	New England Biolabs	C2984I	Subcloning of CXCR7
Reagent	T4 DNA Ligase	New England Biolabs	M0202S	Subcloning of CXCR7
Reagent	Quick Blunting™ Kit	New England Biolabs	E1201S	Subcloning of CXCR7
Reagent	Calf Intestinal Phosphatase	New England Biolabs	M0290	Subcloning of CXCR7
Reagent	NheI-HF	New England Biolabs	R0131S	Subcloning of CXCR7
Reagent	AgeI-HF	New England Biolabs	R3552S	Subcloning of CXCR7
Reagent	NcoI-HF	New England Biolabs	R3191S	Subcloning of CXCR7
Reagent	XbaI	New England Biolabs	R0145S	Subcloning of CXCR7
Supply	Wizard® Plus SV Minipreps DNA Purification System	Promega	A1470	Subcloning of CXCR7
Supply	NucleoSpin® Gel and PCR Clean-up	MACHEREY-NAGEL	740609.50	Subcloning of CXCR7
QPCR reagent	High-Capacity cDNA Reverse Transcription Kit	Applied Biosystems	4368814	QPCR
QPCR reagent	Fast SYBR™ Green Master Mix	Applied Biosystems	4385612	QPCR
PCR reagent	Taq DNA Polymerase	New England Biolabs	M0267S	PCR
Cell viability assay reagent	CellTiter-Glo® Luminescent Cell Viability Assay	Promega	G7572	Cell Viability Assays
Cell culture media and supplements	DMEMF-12, HEPES	Gibco	11330057	Cell culture
Cell culture media and supplements	Penicillin-Streptomycin (10,000 U/mL)	Gibco	15140122	Cell culture
Cell culture media and supplements	B-27™ Supplement (50X), serum free	Gibco	17504044	Cell culture
Cell culture media and supplements	N-2 Supplement (100X)	Gibco	17502048	Cell culture
Cell culture media and supplements	Accutase® Cell Detachment Solution	CORNING	25-058-CI	Cell culture
Cell culture media and supplements	Animal-Free Human FGF-basic (154 a.a.)	Peprotech	AF-100-18B	Cell culture

Cell culture media and supplements	Animal-Free Recombinant Human EGF	Peprotech	AF-100-15	Cell culture
Inhibitors	1,1'-[1,4-PHENYLENEBIS(METHYLENE)]BIS[1,4,8,11-TETRAAZACYCLOTETRADECANE] HCL (1:8)- AMD3100	Asta-Tech	A11761	CXCR4 inhibition
Inhibitors	CCX771	Chemocentrix	N/A	CXCR7 inhibition
Transfection reagent	Polybrene 10 mg/ml	Millipore	TR-1003-G	Lentiviral transduction of GSCs
RNA extraction	Quick-RNA™ Microprep Kit	Zymo Research	R1051	RNA extra

Supplementary Table 2. Primer sequences

Name	Sequence	Gene	Species	Genebank #	Experiment used
Cxcr4 F	CGTTTGGTGCTCCGGTAA	*Cxcr4*	mouse	NM_009911	QPCR
Cxcr4 R	GCCGACTATGCCAGTCAAGAA	*Cxcr4*	mouse	NM_009911	QPCR
Cxcr7 F	GCAGAGGACACCCCACAAATC	*Cxcr7*	mouse	NM_001271607	QPCR
Cxcr7 R	GTCAGAGTAGTTGCCAGGCT	*Cxcr7*	mouse	NM_001271607	QPCR
Hprt F	GGTTAAGCAGTACAGCCCCAA	*Hprt*	mouse	NM_013556	QPCR
Hprt R	ACTGGCAACATCAACAGGACT	*Hprt*	mouse	NM_013556	QPCR
HCXCR7 F2	TCCAGTGACCAGGAGAAGCA	*CXCR7*	human	NM_020311	QPCR, Sanger Seq.
HCXCR7 R2	CGGCAGGTGAAAGGGATGTA	*CXCR7*	human	NM_020311	QPCR, Sanger Seq.
HCXCR7 F1	ATGGATCTGCATCTCTTCGAC	*CXCR7*	human	NM_020311	Colony PCR, Sanger Seq.
Egfp R1	CTTGTACAGCTCGTC	*EGFP*	Synthetic	N/A	Colony PCR, Sanger Seq.
Egfp R2	TGTCGCCCTCGAACTTCAC	*EGFP*	Synthetic	N/A	Sanger Sequencing
Cxcl12 F	GACGGTAAACCAGTCAGCCT	*Cxcl12*	mouse	NM_021704	QPCR
Cxcl12 R	CCTCGGGGGTCTACTGGAA	*Cxcl12*	mouse	NM_021704	QPCR